DEGREE PROJECT IN ,
SECOND CYCLE, 30 CREDITS
STOCKHOLM, SWEDEN 2020

The Temporal Impacts of Climate Condition on Groundwater Flow Using Numerical Transient Modelling

MALIEHA ZANNAT RAHMAN

KTH ROYAL INSTITUTE OF TECHNOLOGY
SCHOOL OF ARCHITECTURE AND THE BUILT ENVIRONMENT

TRITA ABE-MBT-20560

Abstract

Compiling comprehensive understanding of all the available natural resources is an important task which should be carried out as it holds a crucial role for the next generation's lives. In particular, groundwater is considered as one of the vital resources in providing essential drinking water. Krycklan catchment is a well-monitored catchment in Sweden that is characterized with almost 30% of the world's forest cover and it has a range of data sets stored from 1920. A numerical model with several observational constrains is used in this study to investigate the groundwater flow circulation. The numerical model is developed with Visual MODFLOW Flex 6.1 software to investigate the temporal effects of the climate condition on the groundwater flow of the Krycklan catchment through a transient-state condition. Daily precipitation and daily evapotranspiration data along with stream data are used to represent the climatic boundary conditions. The impact of climatic condition on groundwater flow was investigated using two different metrices: groundwater level, and groundwater flow travel time reaching the stream network. The results clearly indicated the variability in groundwater level due to the impact of climatic condition in which the winter and summer months have the highest and lowest groundwater levels, respectively. In addition, the particles tracing results show that physical characteristics of the stream channel substantially influence the shallow groundwater travel time.

Key words: Climatic Condition, Groundwater Flow, Transient-State Modelling, Numerical Modeling, Krycklan Catchment, Visual MODFLOW Flex

Acknowledgements

First of all, I would like to thank my examiner, Anders Wörman (Head of division, Resources, Energy and Infrastructure), for choosing me to be one of his master students and giving me this opportunity to write my thesis with him which has been a dream of mine since I attended his first lecture. Secondly, I would also like to thank my supervisor, Brian Mojarrad (Doctoral student, Resources, Energy and Infrastructure) for guiding me through each and every step of the entire journey and for his unlimited patience with all my questions and inquiries. His enriched knowledge of the numerical modelling process and his passion for research and hydrology has helped me gain a lot of learning experience. I would also like to thank Hjalmar Laudon (Professor, Department of Forest Ecology and Management) for continually helping me out with the data sets from the Krycklan catchment. Lastly, I would like to thank my family for their encouragement and support from hundreds of miles away, that has led me to come this far in my life; I hope to make them proud.

Table of Contents

List of Figures

List of Tables

1. Introduction

Groundwater is an imminent source of fresh water as 98% of earth's available fresh water comes from groundwater which is mainly recharged from precipitation. Streams, rivers, and lakes are the main sources of surface water which constitutes of 80% of daily water consumption while groundwater can sustain these streams and rivers even when there has been no precipitation (USGS, 1984).

Climate change describes a shift in the average conditions such as temperature and rainfall in a region over a long period of time due to increasing greenhouse effect (*What is climate change*, 2020). In general, climate change occurs naturally, but human population growth and associated land-cover conversion (e.g., deforestation) and burning of fossil fuel have substantially accelerated the increase of greenhouse gases (Wu et al., 2012). Rapid climate change has been affecting the world's atmosphere as well as the groundwater system (Gomez Peña, 2017). According to Darwin (2010), fluctuations in temperature and rainfall during a year will have direct impact on changes in groundwater level. Hence, it is essential to understand and analyze the groundwater flow.

The implications of anticipated climate change are difficult to measure and quantify not only at the global scale but also at regional and local levels. In order to study the groundwater flow, groundwater modelling has been used in quite many researches so far (Baalousha, 2008). Numerical simulation models provide the most effective way to estimate the quantity and quality of water exchange between aquifers and surface-water bodies and thereby to quantify the impact of groundwater abstraction (i.e., pumping) and climate change on groundwater systems. Recent studies have demonstrated that hydrological changes and climate change impacts on groundwater can be evaluated with both statistical tools (McCuen 2003; Chen et al. 2002) and complex distributed models (Scibek et al. 2007; Jyrkama and Sykes 2007).

A groundwater model delivers a quantitative framework for synthesizing field information and for conceptualizing hydrogeologic processes (Anderson, et al., 2015). There has been multiple softwares in use for the numerical groundwater modelling such as: Visual MODFLOW, GMS, COMSOL, FEFLOW etc. This study was done using Visual MODFLOW Flex 6.1, which is a research/industry-standard software for modelling groundwater flow and contaminant transport, essential analysis and calibration tools, and provides impressive 3D visualization.

This study simulates the Krycklan catchment groundwater flow, situated in the boreal regions of northern Sweden, in the Västerbotten county. The Krycklan catchment has undergone numerous researches in different disciplines such as hydrology, biology, chemistry, etc. (Laudon et al., 2013; Jutebring Sterte, 2016; Mojarrad et al., 2019a). It is a 68 km^2 watershed catchment that covers the natural mosaic of boreal landscapes consisting of forests, mires, streams, and lakes that characterizes 70% of the area in Sweden, which is representative of 30% of the world's forest cover (Laudon, 2017). There are almost 500 scientific articles based on data from Krycklan. The goal of these studies at Krycklan is to create better methods and models to predict how nature will look in the future under changing conditions such as a warmer climate (*Hydrological Research at Krycklan Catchment Study*, 2020).

In this study, a numerical model of the catchment was developed to analyze the groundwater flow circulation and how it is affected by the climatic changes (precipitation, evaporation, etc.) over a year (i.e., 2019). The numerical model was implemented with monthly recharge data and measured constant stream data to characterize the catchment groundwater flow. In addition, the numerical model was manually calibrated with respect to the initially assumed hydraulic conductivities of the soil types based on the hydraulic head results found at the end of the model run.

1.1 Aims & Objectives

The principal aim of the study is to achieve an enhanced understanding of the groundwater flow of the Krycklan catchment and how it is affected by the temporal effects of the climate condition over a year (2019) through a transient state model. The detailed objectives of the study are as follows:

- Collect the daily meteorological data, high resolution topographical data, hydrological stream data, and relative catchment shapefiles to represent the catchment and its characteristics as detailed as possible
- Create a conceptual model of the study catchment based on the collected data
- Convert the conceptual model into a numerical model with a well-defined grid size so that the model results represent reality of the catchment
- Assess the model results and calibrate the model accordingly
- Appraise the final findings and reflect upon the potential improvements of the numerical model
- Gain a better insight on the operations and possibilities of the Visual MODFLOW Flex 6.1 for future work with groundwater modelling

1.2 Study Area

The study area, known as the Krycklan catchment, is located in northern Sweden in the Västerbotten county, north-west of Umeå city (64°,14'N, 19°46'E) (Laudon, et al., 2013). Figure 1 shows the catchment boundary, which is surrounded by mountains, namely, Näverliden, Buberget and Ö Kryckeltjärn in the east; Koverberget and Abborrtjärn in the north-west; and lastly, Mullkälen, and Riskälen in the south (Jutebring Sterte, 2016). Krycklan is a tributary to the national Vindelälven River which starts in the mountain, crosses Sweden, and enters the Baltic Sea near Umeå city (*Hydrological Research at Krycklan Catchment Study*, 2020). There are several streams and small lakes in the catchment area as well (Figure 2). The main streams are namely, Åhedbäcken, Långbäcken, Nymyrbäcken and Krycklan. (Jutebring Sterte, 2016)

The Krycklan catchment is partially situated in the Svartberget experimental forests established in 1920 which currently is a unit of the Swedish University of Agricultural Sciences (SLU). Due to the very accessible and advanced long-term data stored from the experimental parks, there are over 1000 scientific publications and 98 Ph-D theses that contained results from Svartberget since the

early days of its establishment. Also, it is assumed that almost half of the results are from the Krycklan catchment (*The Krycklan Infrastructure*, 2020).

There are 18 partly nested sub-catchments which make Krycklan Catchment Study (KCS) an advanced field research infrastructure (Figure 2). Each of these sub-catchments have monitoring/research stations. Among these sub-catchments, C7 was built in 1980 as a research catchment, two more were built in 1984 namely C2 and C4, and then finally the remaining were constructed in 2002. There are readily available daily discharge data along with climate data, groundwater and stream water chemistry, and many more from these sub-catchments in the https://franklin.vfp.slu.se/ website that have been collected from these research stations over a very long period of time. Along with the Krycklan website, the SGU and SMHI websites have also been used from time to time for data collection.

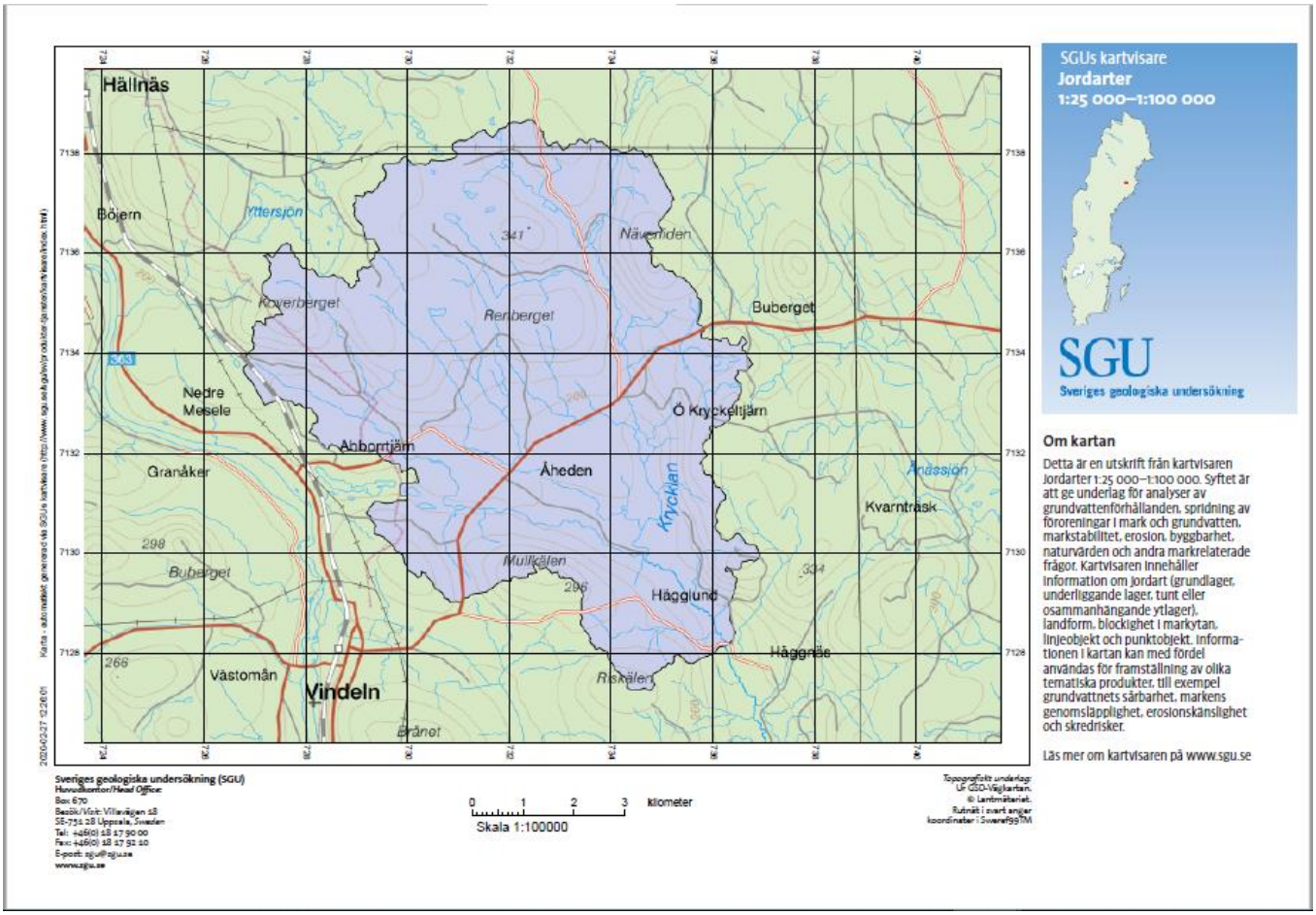

Figure 1: Model domain (Krycklan Catchment) in the shaded area (©Sveriges geologiska undersökning (SGU))

The Krycklan catchment has multiple climate monitoring sites that have been active since 1980 as a part of a reference monitoring system (figure 5) (Laudon, et al., 2013). The names of the sites are respectively Stortjäm, Hygget, and Heden from upstream to downstream. The Hygget and Heden sites were established in 1980 while the Stortjäm site was established in 2016.

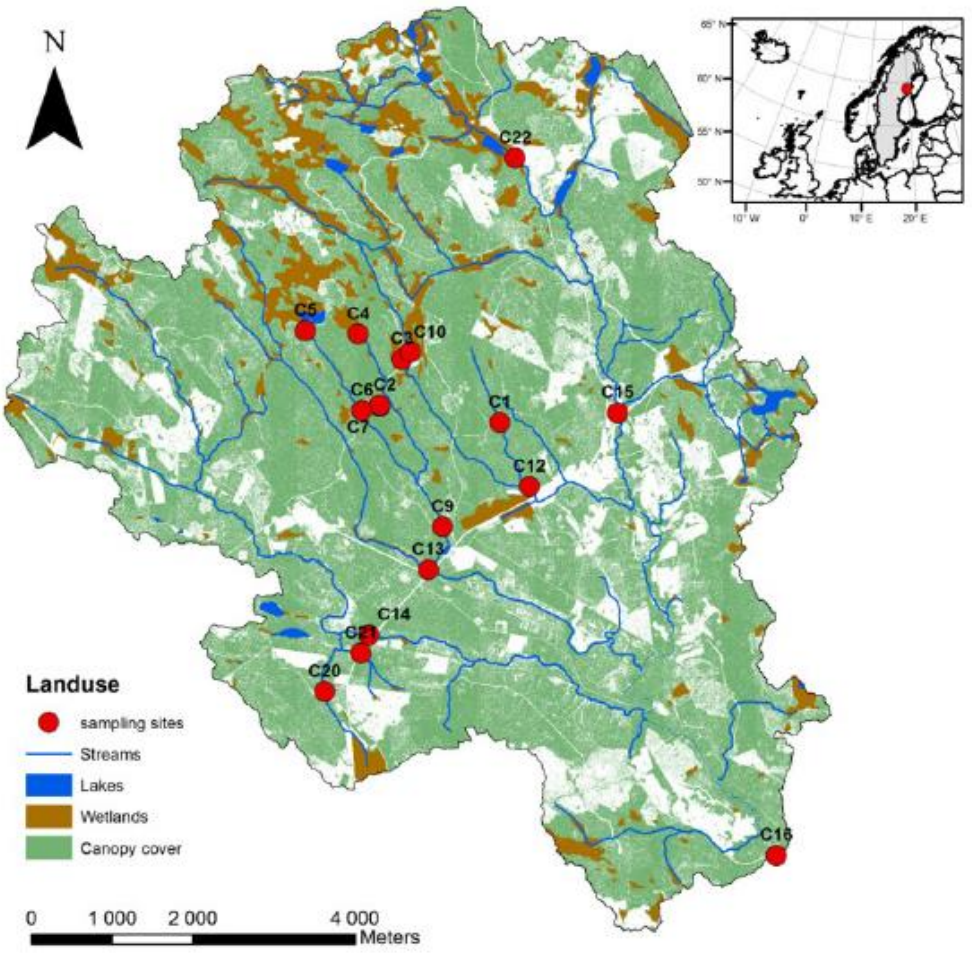

Figure 2: Area map of Krycklan Catchment Study (KCS) with lakes, streams, and sampling/ research sites (Laudon, 2017)

1.2.1 Topographical Data

Visual MODFLOW Flex 6.1 uses raw GIS data to form a conceptual model from scratch. The study collected the following raw GIS data shapefiles from the Krycklan website as topographical data-

- Krycklan Outline: the watershed boundary
- Regular Catchments: the outline of the sub-catchments
- DEM Krycklan 2m: the 2×2 meter DEM of the catchment
- Soil type: the heterogeneity in quaternary deposits map of the catchment
- 5 ha streams: the raster representation of the stream network

The elevation of the catchment ranges from 114-405 meter above sea level (a.s.l) (Mojarrad et al., 2019a). Figure 3 and figure 6 show almost 51% coverage of till in the whole catchment, especially in upstream of the catchment which is convoluted with peat near the stream network while the soil gradually replaced with clay-silt and postglacial sedimentary deposits in downstream part of the catchment. This uniqueness that divide the topography of the catchment into two distinct parts is due to the creation of the highest postglacial coastline that traverse the catchment at 257 meter a.s.l approx. as the catchment is undergoing iso-static rebound following the last deglaciation (Laudon, et al., 2013).

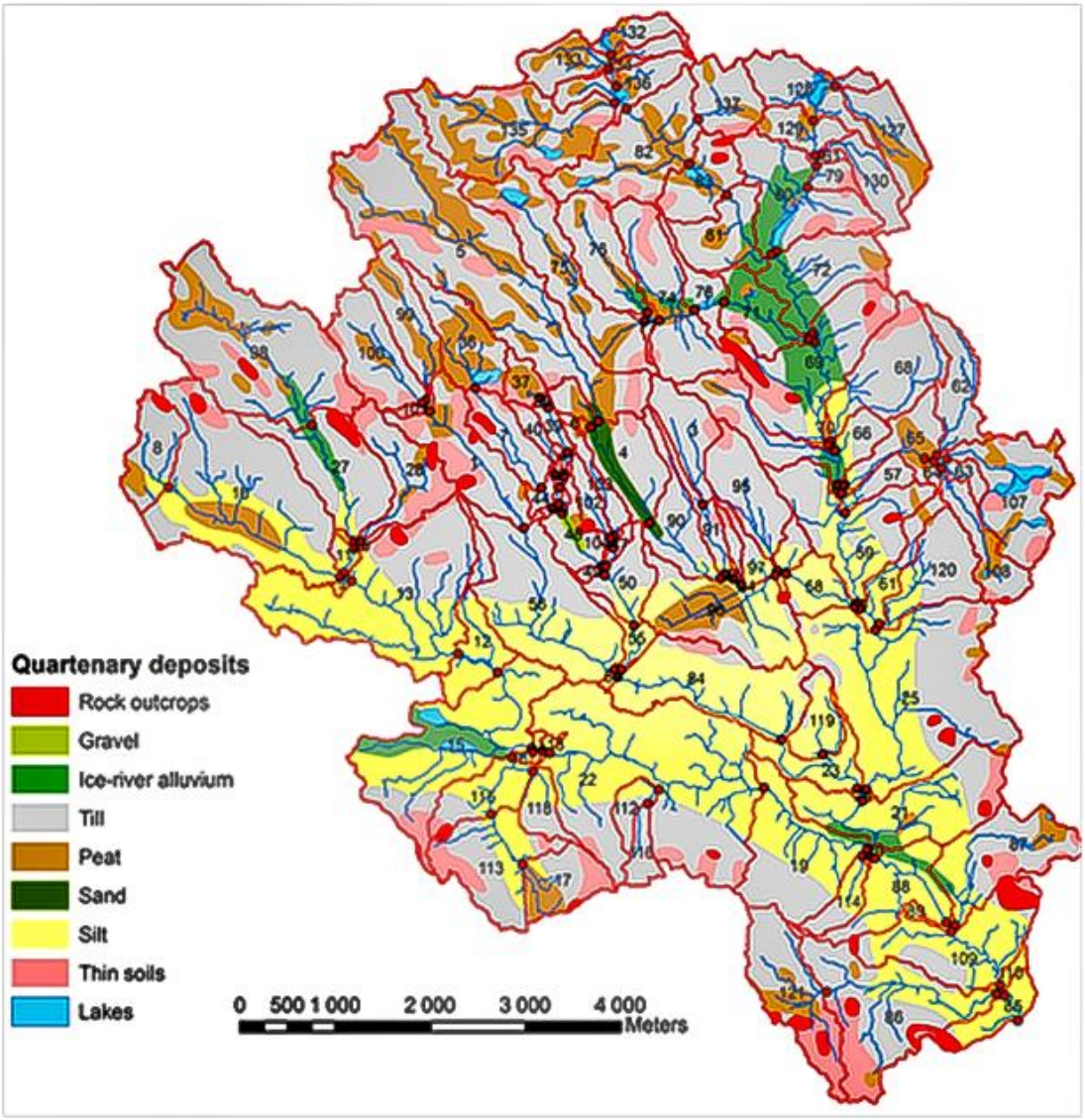

Figure 3: The soil type map of the Krycklan Catchment (Laudon, et al., 2013)

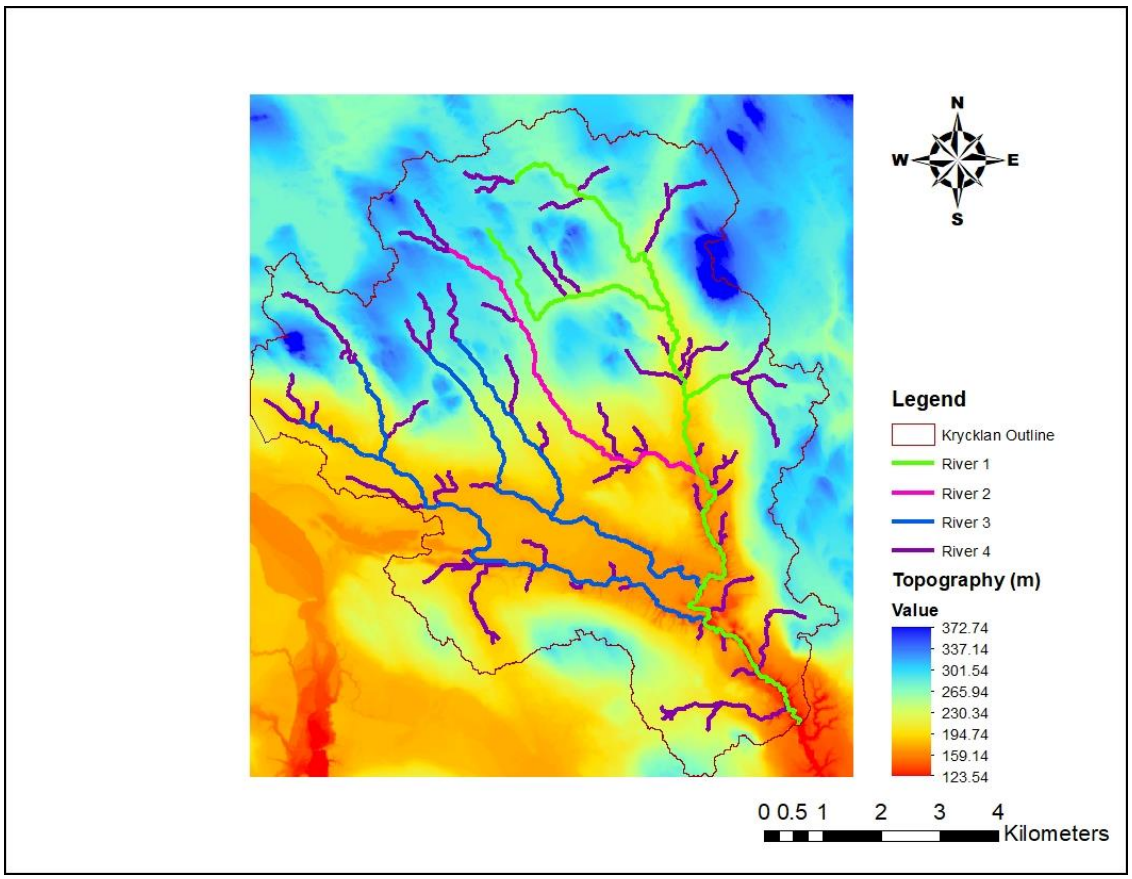

Figure 4: Topography elevation variation over Krycklan catchment

The stream network of the catchment has been split into four groups (where group 1,2, and 3 are the main streams and group 4 represents the tributaries) so that the model is more practical and similar to the real environment as they would vary in values for river width, height, water depth, etc. This division helped input of individual data for each stream group in the model. The division is performed with regard to the study sites classification of Jaremalm and Nolin (2006) which can be seen in figure A-1 and table A-1 in the Appendix. The topographical surface layer is assigned as the river bottoms and the river stages are assigned to the especially modified topographical surface layer with added individual water depth height of each group. The river conductance has been considered to be 1E-04 (Morén et al., 2017; Mojarrad, et al., 2019a).

Figure 4 illustrates the stream network within Krycklan catchment. The main streams are Nymyrbäcken (river 2), Långbäcken (river 3), Åhedbäcken (river 3), and Krycklan (river 1) from upstream to downstream, respectively. The physical characteristics of the stream used as the river boundary conditions of the model are taken from Jaremalm and Nolin (2006). The conceptual model for the climatic conditions is designed in transient state, however, due to lack of monthly stream cross-section data, the river boundary conditions has been considered to be in a steady state which is shown in table 1.

Table 1: River boundary data

River No.	Stage (m)	Bottom (m)	Riverbed Thickness (m)	River Width (m)	Riverbed Conductance (m/s)
1	Surface elev. + 0.31	Surface elev.	1	4.78	1E-04
2	Surface elev. + 0.29	Surface elev.	1	1.03	1E-04
3	Surface elev. + 0.24	Surface elev.	1	0.86	1E-04
Tributaries	Surface elev. + 0.11	Surface elev.	1	0.53	1E-04

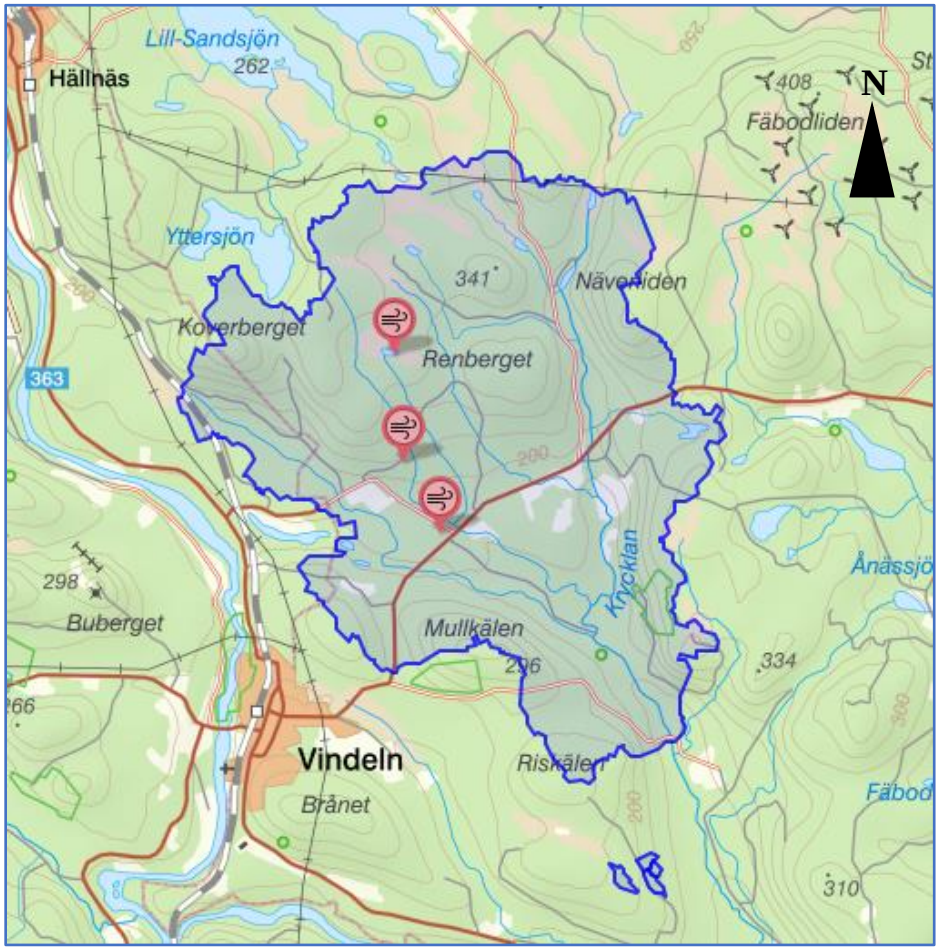

Figure 5: Climate Monitoring stations in the Krycklan catchment marked with pins

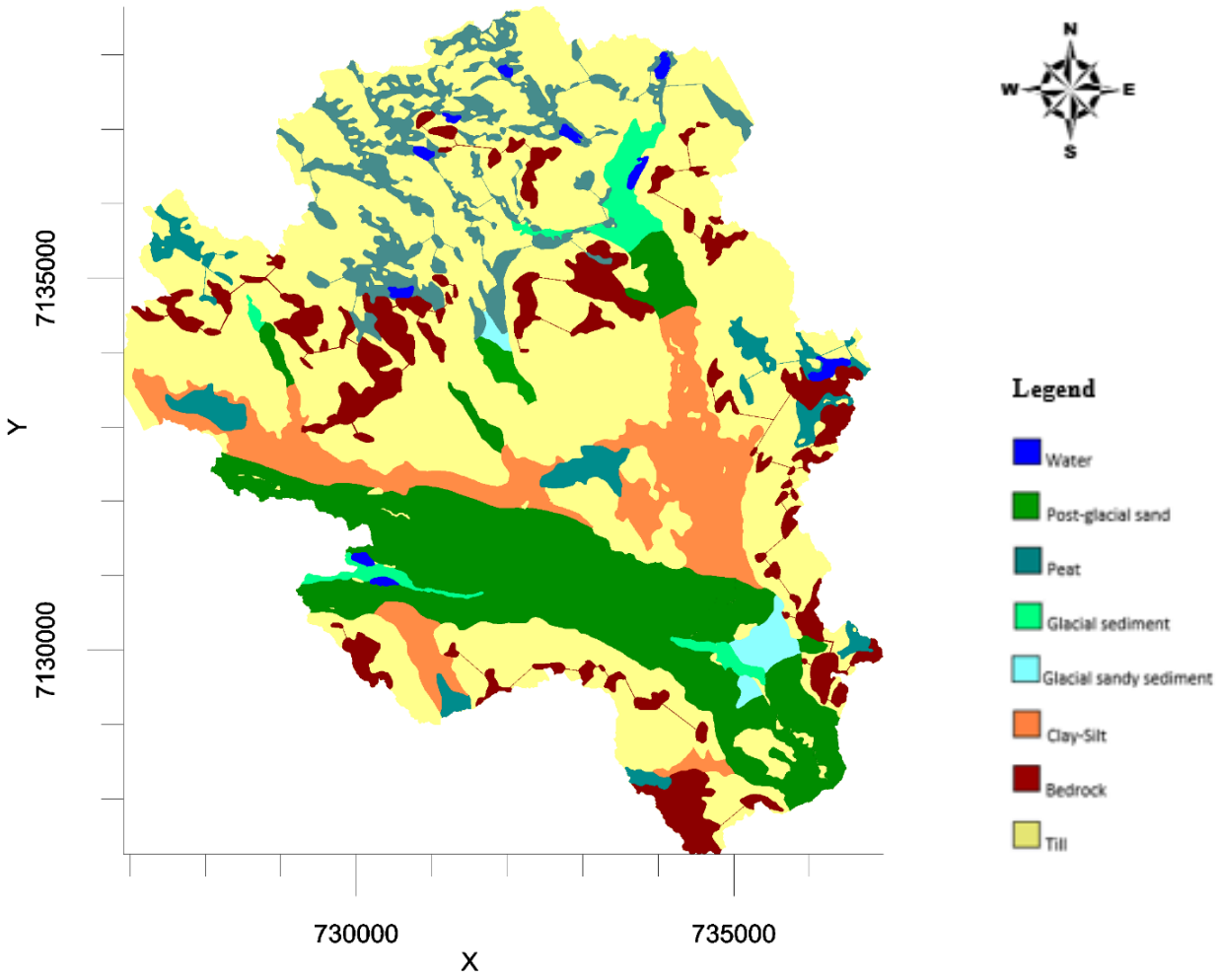

Figure 6: Soil type map constructed on VMOD Flex 6.1

2. Background Theory and Literature Review

This study applies the physical characteristics of the hydrological cycle of the Krycklan catchment into Visual MODFLOW Flex in order to create a conceptual model of the real environment which is then converted into a numerical model. The whole process of modelling can be a little intricate as the hydrology of a region is determined by its weather patterns and by physical factors such as, topography, vegetation, and geology (Chow, et al., 1988). So, this section is here to provide some background theory of the basic and important hydrological processes related to the study, and some information to get to know about the software, and also to discuss a few previous studies done on the catchment or on numerical groundwater modelling as well.

2.1 Hydrologic cycle

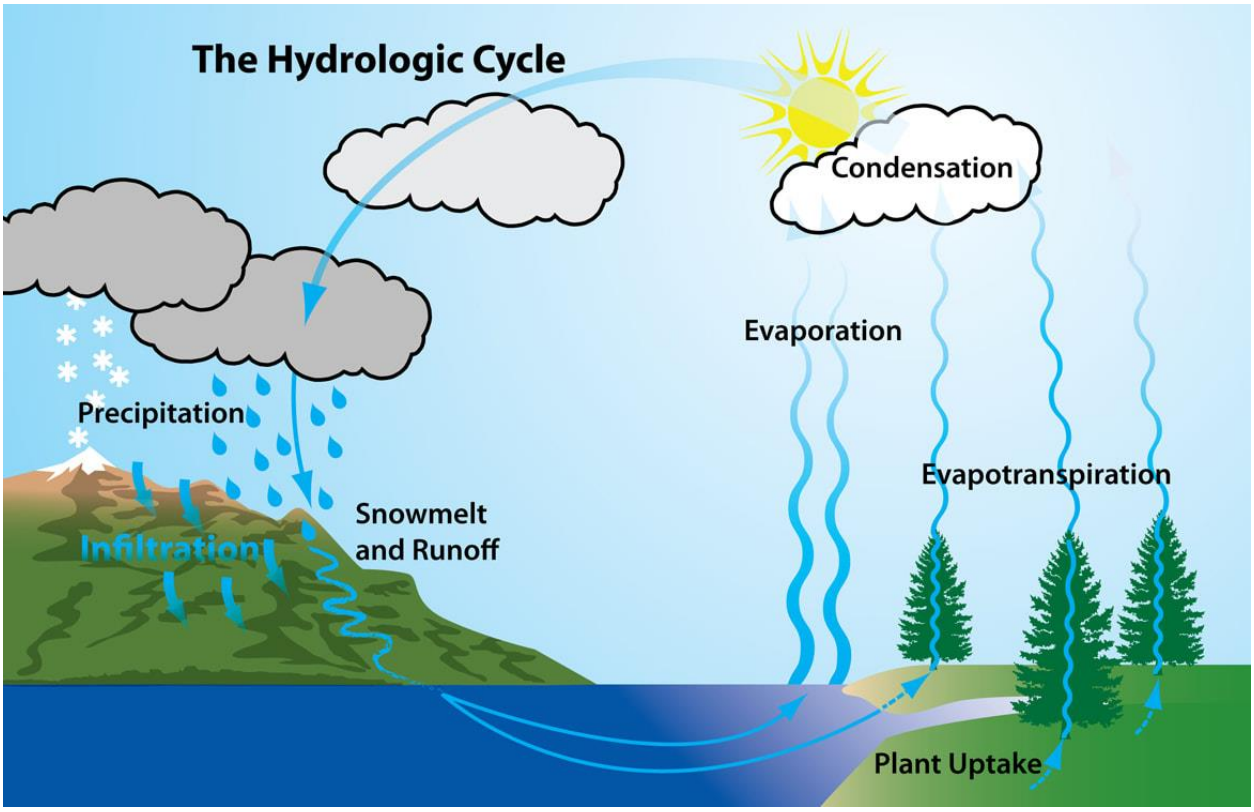

Figure 7: The hydrologic cycle (https://notesychs.weebly.com/the-hydrological-cycle.html)

The hydrologic cycle, which has no beginning or end and whose many processes are occurring continuously, is the central focus of hydrology (Chow, et al., 1988). The hydrologic cycle (figure 7) can be viewed as a natural machine, a constantly running, distillation and pumping system. The primary source of energy for the operation of this machine is the Sun that supplies heat energy (P. Singh, 2017). The main elements and processes of the hydrological cycle is described below.

2.1.1 Precipitation

Precipitation includes rainfall, snowfall, drizzle, graupel, hail, sleet and other processes through which water falls to the ground. Precipitation is formed by the lifting of an air mass in the atmosphere in order for it to cool down and some of its moisture to condense (Chow, et al., 1988). Precipitation happens when a part of the atmosphere gets saturated with water vapor meaning reaching 100% relative humidity, so that the water condenses and precipitates (*Precipitation*, 2020). The process of precipitation is well-illustrated in figure 7. It can be seen that as the water evaporates from the surface and also transpirated from the vegetation, it condenses in the clouds and changes its state from vapor to liquid.

2.1.2 Evapotranspiration

Evapotranspiration is a combined term for two hydrological processes simultaneously occurring together (Figure 7) which are evaporation and transpiration. Evaporation happens when the surface loses water as vapour whereas transpiration occurs when water is lost from the crops or vegetation. These loss of water is taking place mainly due to the solar radiation along with other environmental elements. In the absence of any supply of water to the soil surface, evaporation decreases rapidly and may cease almost completely within a few days (Allen, et al., 1998). The rate of evapotranspiration is affected differently by each of the elements considering the stage of a crop. The evapotranspiration rate can depend 100% on evaporation at the sowing stage of a crop while it can depend 90% on transpiration once the crop is fully grown (Allen, et al., 1998). Hence, it is important to consider all the factors such as- crop type and development stage, wind speed, solar radiation, air temperature and humidity etc.- in calculation of evapotranspiration which leads to different kinds of evapotranspiration. Usually the available evapotranspiration data (in many data bases) reflect the potential or reference evapotranspiration. The crop or actual evapotranspiration can be estimated by the following equation (Allen, et al., 1998).

$ET_c = K_c \times ET_o$ ……...……. (1)

where, ET_c is the crop evapotranspiration, ET_o is reference evapotranspiration, and K_c is crop co-efficient.

ET_c is defined with a crop coefficient methodology while ET_o is integrated with the effects of different weather conditions and the characteristics of the crop. In addition, averaged impacts of soil evaporation are incorporated into K_c (Allen, et al., 1998).

2.1.3 Infiltration

The process of water penetrating from the ground surface into the soil is known as infiltration (Chow, et al., 1988). Part of this water might penetrate deep into the underground (saturated zone) while part of it might stay at root depth (unsaturated zone) where it can be used by the plants. There are many factors affecting the infiltration rate such as- precipitation, base flow, soil characteristics, porosity, hydraulic conductivity, land cover, soil moisture content, and evapotranspiration. However, through a simplified approach i.e. by disregarding the unsaturated zone and the time taken for the water to reach the saturated zone due to small difference between the ground surface and the groundwater surface, the infiltration concept can be presented as:

Infiltration = Precipitation – Evapotranspiration ..... (2)

The process of infiltration helps to naturally recharge the groundwater over a period of time. It recharges the deep aquifers and help maintain the natural groundwater level.

2.1.4 Groundwater Flow

Groundwater is a very important provider to many stream and river flows, especially in the dry season when precipitation is scarce (Mojarrad et al., 2019a). There are two zones below the ground

surface, which are, unsaturated zone and saturated zone. Water is typically stored within the unsaturated zone in the cracks and spaces of rocks, pores of sand and soil for plant intake and such. The saturated zone is found below the water table where flow of groundwater takes place. The groundwater flow can be defined as the portion of streamflow which infiltrates the ground surface and enters the phreatic zone and gets discharged into a stream channel, or springs and seepage water (*Groundwater flow*, 2020). Darcy's law is the governing equation in saturated porous media which is used to calculate the flow velocity. The Darcy's law is as follows (Chow, et al., 1856).

$$q = -K \times \nabla H \quad \text{.....(3)}$$

where, q is Darcy velocity vector (L/T), K is the hydraulic conductivity (L/T),

∇ is nabla operator, and H is the hydraulic head (L).

2.2 Numerical Groundwater Modelling

One of the most effective means for the investigation of groundwater management and remediation is groundwater modelling (Baalousha, 2008). A model is a representation of a complex reality in a simplified way for the purpose of analysis of present phenomena or to predict future behavior (Baalousha, 2008). To achieve a realistic groundwater model, mathematical modelling should be performed at the beginning of the hydrogeological study that addresses the nontrivial questions (Bredehoeft, et al., 1995). As Hill (2006) mentioned, it is proposed to start with a simple model as long as the model concept satisfies the modelling objectives, and then the complexity of the model can gradually be increased. The reliability of a numerical model depends on the accuracy of the conceptual model as it summarizes the hydrogeological information of the modelled site (Lekula, et al., 2018).

A groundwater model of the Northern Cities Management Area (NCMA) of Santa Maria groundwater basin was created by Wallace, B. M. (2016) where transient aquifer inflow and outflow of the area were evaluated using USGS MODFLOW-2005/PEST and an improved safe yield value was identified for better aquifer management in the future.

The Krycklan catchment located in the northern Sweden was characterized with an aim of aiding future researches regarding characterization of the catchments ground and surface water flow (Jutebring Sterte, 2016). An integrated model software tool has been used in the study called MIKE-SHE. The study resulted with a manually calibrated model that captured the water flow dynamics of the catchment. The heterogeneity in hydraulic conductivity of the numerical model was calibrated and verified as well.

The coastal salinity intrusion status of groundwater was investigated with Visual MODFLOW in Khulna, Bangladesh. A numerical model was developed and further validated with collected field data which had striking resemblance to the model results (Ahsan, 2019). The results showed 3.75 times increase in the salinity concentration in a period of 20 years.

A 3D transient groundwater model was created using Visual MODFLOW for the Luancheng region of the North China Plain. The model resulted in establishing a major association of the agricultural water use with the decrease in the piezometric surface which took place due to the

excessive pumping of aquifer water and deplete in the unconfined water table by half meter per year (Jia, et al., 2002).

These studies along with hundreds of more show that effective groundwater modelling helps in the decision making process of current projects, and future predicaments without having to establish a project in reality.

2.3 Visual MODFLOW FLEX 6.1

Visual MODFLOW or VMOD Flex is a research/industrial standard, easy to use tool that unites codes for various groundwater simulations, e.g. groundwater flow, contaminant transport, essential analysis and calibration tools with a remarkable 3D visualization facilities (*Visual MODFLOW Flex*, 2020). This software is quite famous among the groundwater modelers around the world for assessing different sorts of local and international groundwater related problems.

VMOD Flex uses raw GIS data objects in order to build a 3D groundwater conceptual model and numerical model. Firstly, to build a conceptual model of a groundwater system, all the relevant GIS raw data files are imported into the software, e.g. geologic formation structures, hydrogeologic properties, boundary conditions etc. and they are designed outside the model grid which provides a flexibility to modify the groundwater system's interpretation before converting to a numerical model (Visual MODFLOW Flex 6.1, 2019).

VMOD Flex allows the user to translate the conceptual model into more than one numerical model that will run in the groundwater modeling engine. Multiple numerical model runs can be performed for a single groundwater system which opens up more opportunities to analyze the groundwater flow mechanism of a model area. There is a separate workflow generated for each type of numerical model. There are mainly two types of grids that can be generated for workflows, structured finite difference grids or unstructured grids for numerical workflow and USG workflow, respectively. The structured finite difference grid works with different flow engines such as – MODFLOW-2000, -2005, -NWT, -LGR, -SURFACT, SEAWAT, MT3DMS, and RT3D (Visual MODFLOW Flex 6.1, 2019).

This study was done using the MODFLOW-2005 flow engine. MODFLOW was originally created exclusively as a groundwater flow model. Then, it evolved into MODFLOW-2000 with different time and needs from the program, and finally turns into MODFLOW-2005. MODFLOW-2005 works by solving the following three-dimensional equation of movement of ground water of constant density thorough porous earth material (Harbaugh, 2005),

$$\frac{\partial}{\partial \mathrm{x}}\left(K_{xx}\frac{\partial \mathrm{h}}{\partial \mathrm{x}}\right)+\frac{\partial}{\partial \mathrm{y}}\left(K_{yy}\frac{\partial \mathrm{h}}{\partial \mathrm{y}}\right)+\frac{\partial}{\partial \mathrm{z}}\left(K_{zz}\frac{\partial \mathrm{h}}{\partial \mathrm{z}}\right)+W=S_s\frac{\partial \mathrm{h}}{\partial \mathrm{t}} \quad \text{.....(4)}$$

Where,

K_{xx}, K_{yy}, and K_{zz} are hydraulic conductivity values along x, y, and z axes respectively, which are assumed to be parallel to the major axes of hydraulic conductivity (L/T);h is potentiometric head (L),W is volumetric flux per unit volume representing sources and/or sinks of water, with W< 0.0

for flow out of the groundwater system, and W> 0.0 for flow into the system (T^{-1}), S_s is specific storage of the porous material (L^{-1}), T is time (T).

Equation 4 describes the groundwater flow under nonequilibrium conditions in a heterogeneous and anisotropic medium, provided the principal axes of hydraulic conductivity are aligned with the coordinate directions. The analytical solutions for this equation are only possible for very simple systems. Thus, there is a need to utilize different numerical methods to acquire approximate solutions. MODFLOW-2005 solves this equation with the finite difference method. In this method, the continuous system of equation 4 is replaced by a finite set of discrete points in time and space and the partial derivatives are replaced by terms calculated from the head difference values at each joint (Harbaugh, 2005).

The discretization of the hydraulic heads is done spatially with respect to the x, y, and z grid directions with unit vectors i, j, and k. Each direction in space and time is discretized with variables, Δr_j, Δc_i, and Δv_k for the i, j, and k directions in MODFLOW. The final outputs or results from a model run are heavily influenced by the discretization. If the discretization is too coarse, the results will be overestimating by averaging the important factors while if the discretization is too fine, it will result in a finer model resolution with more acceptable results but it will consume a lot of time and computational resources (Wallace, 2016). However, the very fine resolution would affect the groundwater flow velocity. Marklund and Wörman (2011) showed that 70 m is the optimum resolution for the numerical grid.

In this study, the grid size is specified with rows, columns, and layers are known as NROW, NCOL, and NLAY respectively in the grid. This grid in MODFLOW is assumed to be rectangular horizontally and can be distorted vertically, see figure 8 (Harbaugh, 2005). MODFLOW uses the principle of the conservation of mass along with Darcy's law to solve the groundwater flow equation while assuming constant groundwater density and gets the following finite difference solution (eq. 5) for a hydraulic head $h^m_{i,j,k}$ at nodes i, j, and k for time m where CR, CC, and CV are the hydraulic conductance variables in i, j, and k directions respectively (Wallace, 2016).

$$CR_{i,j-\frac{1}{2},k}\left(h^m_{i,j-1,k} - h^m_{i,j,k}\right) + CR_{i,j+\frac{1}{2},k}\left(h^m_{i,j+1,k} - h^m_{i,j,k}\right) + CC_{i-\frac{1}{2},j,k}\left(h^m_{i-1,j,k} - h^m_{i,j,k}\right) + CC_{i+\frac{1}{2},j,k}\left(h^m_{i+1,j,k} - h^m_{i,j,k}\right) + CV_{i,j,k-\frac{1}{2}}\left(h^m_{i,j,k-1} - h^m_{i,j,k}\right) + CV_{i,j,k+\frac{1}{2}}\left(h^m_{i,j,k+1} - h^m_{i,j,k}\right) + P_{i,j,k}h^m_{i,j,k} + Q_{i,j,k} = SS_{i,j,k}(\Delta r_j \Delta c_i \Delta v_{k)}\left(\frac{h^m_{i,j,k} - h^{m-1}_{i,j,k}}{t^m - t^{m-1}}\right) \quad \text{..} (5)$$

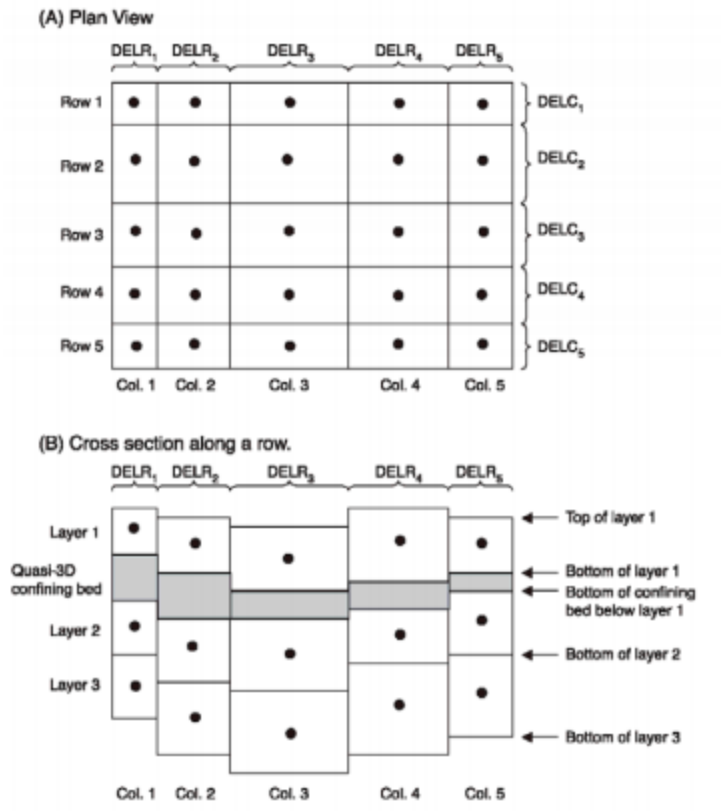

Figure 8: A discretized MODFLOW finite difference grid (Harbaugh, 2005)

MODFLOW uses iterative methods to attain solution for the finite difference equation for each time step. The head value calculations for end of a time step is initiated with the approximation of a trial head value and then starting a procedure of calculation that alters the estimated head values and produces a new set of head values that matches the equation argument the closest which are then replaced by the new set of head values which repeats the calculation creating more satisfactory set of head values after each iteration (Harbaugh, 2005).

VMOD Flex provides different kinds of solver to solve numerical equations in the flow engines. These are-

- PCG2: Preconditioned Conjugate-Gradient Package
- SIP: Strongly Implicit Procedure Package
- SOR: Slice-Successive Overrelaxation Package
- WHS: WHS Solver for VMOD Flex
- GMS: Geometric Multigrid Solver
- SAMG: Algebraic Multigrid Methods for Systems
- AMG: Algebraic Multigrid Solver

Different solver comes with individual setting parameters. The selection of a solver can be done according to the desired outputs of a model and the type of flow engine in consideration.

For this study, The PCG2 solver is used which utilizes the preconditioned conjugate-gradient method in order to solve the produced simultaneous equations of the model. It operates on a two-tier approach to a solution at one time step with inner and outer iterations. The hydrogeologic parameters such as- storativity, transmissivity etc. of the flow system are uploaded in the preconditioned set of matrices in the outer iterations. The inner iterations will stop when the final convergence criteria is met or the number of maximum defined inner iterations are done while the outer iterations continue until the final convergence criteria are met on the first inner iteration after an update (Visual MODFLOW Flex 6.1, 2019).

3. Data and Methods

This section explains the procured data and the methodology of the modelling process.

3.1 Hydrological Data

The heterogeneity in hydraulic conductivities was assumed with account taken to different existing soil type in Krycklan catchment (Figure 6). The initial hydraulic conductivities were assumed according to Jutebring's (2016) study on the Krycklan catchment. These assumed initial hydraulic conductivities were calibrated with respect to the hydraulic heads achieved from the result maps after the model runs multiple times. The calibrated hydraulic conductivities were validated when the resulting hydraulic head map resembled the actual topography of the model domain. The initial and final hydraulic conductivities are given in table 2, where K_x is the horizontal conductivity in the horizontal (x-direction), K_y is the horizontal conductivity in the horizontal (y-direction) and K_z is the vertical conductivity in the vertical (z-direction). The vertical hydraulic conductivity, K_z is generally assumed to be decreased by an order of magnitude from the horizontal conductivities but it is assumed to be equal in some cases for calibration purposes.

Table 2: Initial and final hydraulic conductivity values applied in the modelling process

Soil Type	Initial K (m/s)			Final K (m/s)		
	K_x	K_y	K_z	K_x	K_y	K_z
Bedrock outcrops	1E-10	1E-10	1E-11	1E-8	1E-8	1E-8
Clay-Silt	4E-8	4E-8	4E-9	1E-7	1E-7	1E-8
Post-glacial Sand	1E-4	1E-4	1E-5	1E-5	1E-5	1E-6
Glacial Sediment	1E-5	1E-5	1E-6	1E-4	1E-4	1E-5
Glacial Sandy Sediment	2E-4	2E-4	2E-5	1E-5	1E-5	1E-6
Peat	3E-6	3E-6	3E-7	1E-6	1E-6	1E-7
Water	2E-7	2E-7	2E-8	1E-7	1E-7	1E-8
Till	1E-7	1E-7	1E-8	1E-6	1E-6	1E-6

3.2 Climate Data

The climate data used in this study are the daily precipitation and potential evapotranspiration data. The potential evapotranspiration data is not the actual transpiration data as it does not consider the surrounding crops of an area. The crop's coefficient has to be taken into consideration and the crop evapotranspiration has to be calculated from equation 1. The crop coefficient depends on multiple factors such as- type of crop, climate condition, crop growth stage etc. (Allen, et al., 1998). Krycklan catchment is covered by forest up to almost 90% of its area, the forests are dominated by Scots pine and Norway pine which consists 63% and 26% of the area, respectively; there are also Birch and Spruce trees present in the catchment (Laudon, et a., 2013). Since more than 90% of the trees present in the forest are coniferous, the crop coefficient, Kc is assumed to be 1 for the calculation of the crop evapotranspiration (Allen, et al., 1998). Table 3 shows the monthly infiltration calculation input for the model. Both the daily reference evapotranspiration and precipitation data is collected from the Svartberget reference climate station Hygget (figure 8).

Table 3: Infiltration calculation for the model (Reference: climate monitoring program at SLU experimental forests)

Month	Precipitation mm/day	Reference Evapotranspiration, ETo (mm/day)	Crop coefficient, Kc	Crop Evapotranspiration, ETc (mm/day)	Infiltration mm/month
Jan	0.916129025	0.024193548	1	0.024193548	27.64999979
Feb	1.603571408	0.156071429	1	0.156071429	40.52999943
Mar	2.116129043	0.276451613	1	0.276451613	57.03000032
Apr	0.25333333	1.719	1	1.719	-43.9700001
May	3.125806467	2.635483871	1	2.635483871	15.20000048
Jun	1.480000002	4.200333333	1	4.200333333	-81.60999993
Jul	0.980645158	4.226129032	1	4.226129032	-100.6100001
Aug	2.670967805	2.332903226	1	2.332903226	10.48000196
Sep	1.666666668	0.913666667	1	0.913666667	22.59000003
Oct	1.451612903	0.157419355	1	0.157419355	40.11999999
Nov	1.789999959	-0.074	1	-0.074	55.91999877
Dec	2.161290324	-0.028709677	1	-0.028709677	67.89000003

3.3 Method

The procedure of development of the groundwater model of the Krycklan catchment is explained in this section. The method is divided into three parts: evaluated matrices, conceptual modeling and numerical modeling.

3.3.1 Evaluated Matrices

In order to incorporate the surface water bodies, i.e. the rivers of the catchment into the model, river boundaries have been introduced to the model when assigning boundary conditions. This surface water and groundwater interaction is simulated by the river package of the MODFLOW engine through a seepage layer which divides the surface water body from the groundwater system. River leakance is a conceptual hydrogeological term that is expressed in per unit length. The river leakance is by default calculated in the model by the following formula (Visual MODFLOW Flex 6.1, 2019),

$$L = \frac{RL \times W \times K \times CF}{RBT} \quad \text{..... (6)}$$

Here,

L is the leakage (L^2/T), RL is the reach length (L) of the river line in each grid cell, W is the river width (L) in each grid cell, K is the Riverbed K_z (L/T), CF is a conversion factor, RBT is the riverbed thickness (L).

3.3.2 Conceptual Modeling

The first step of groundwater modeling is the construction the conceptual model of the study domain. A conceptual model should resemble the study area and its surroundings as precisely as possible to reflect a decent realization of the Krycklan catchment. A conceptual model is the depiction of the study area's hydrogeological system. The conceptual model for this study is developed in 8 steps in Visual MODFLOW Flex 6.1.

The modeling objectives are defined where the flow and saturation type are specified according to the model necessity. In this study, the saturation and flow types were saturated (constant density) and groundwater flow, respectively. Then, the required data for the modelling were collected. This is where the raw GIS data mentioned in 1.2.1 are imported into VMOD Flex 6.1. The imported files can be polygons, polyline, surface data, points, etc. The model was stratified into two different layers surrounded by three horizons: the bottom, the bedrock, and the topography surfaces, from bottom to top, respectively (figure 9). Two property zones were defined in-between the three horizons reflecting Quaternary deposits and the bedrock (figure 10). The different soil types, lakes, and rivers are assigned to zone 1 in the define property zone step along with the hydraulic conductivities as mentioned in table 2. Figure 11 shows the boundary conditions of the model. The recharge boundary is a transient-state boundary with a time-series monthly recharge data for 2019

calculated in table 3, and the river boundary is a constant boundary with the non-varying stages through the whole time period.

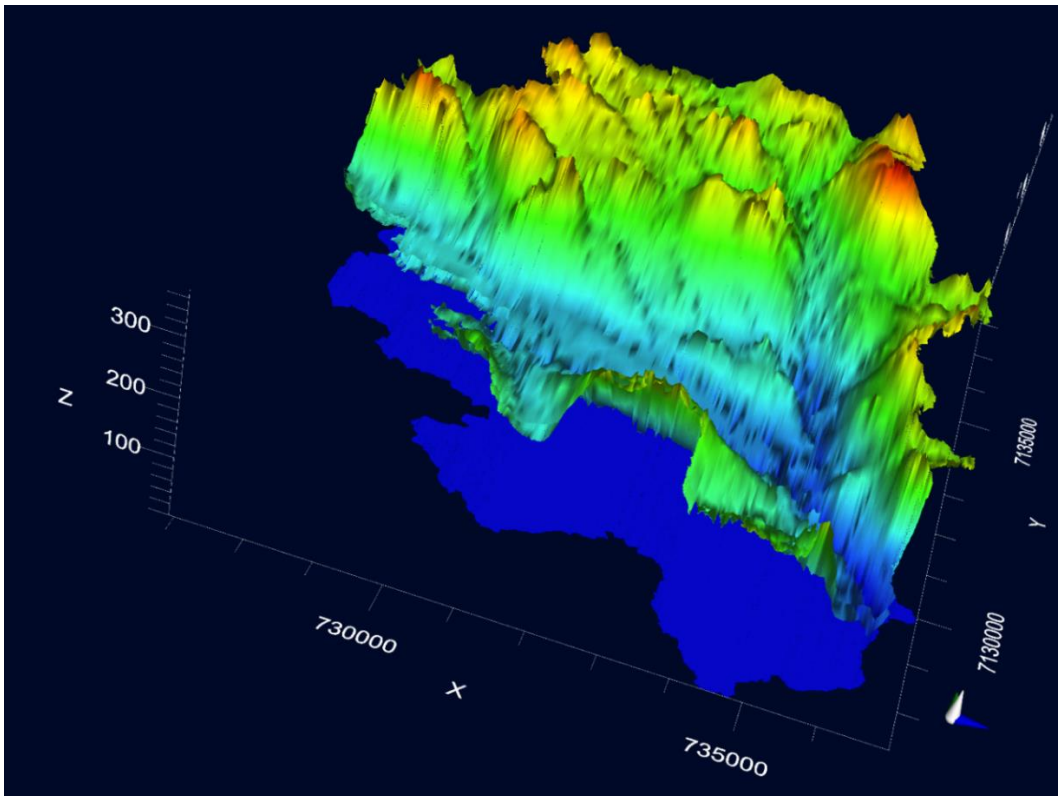

Figure 9: Structural horizons defined in the model

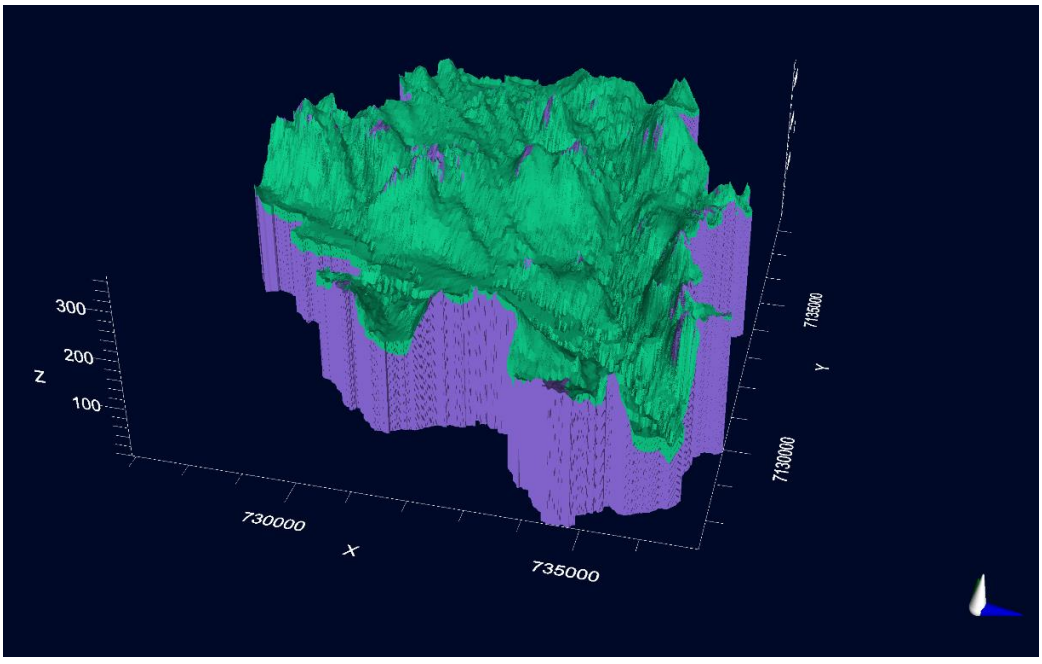

Figure 10: Structural zones defined in the model

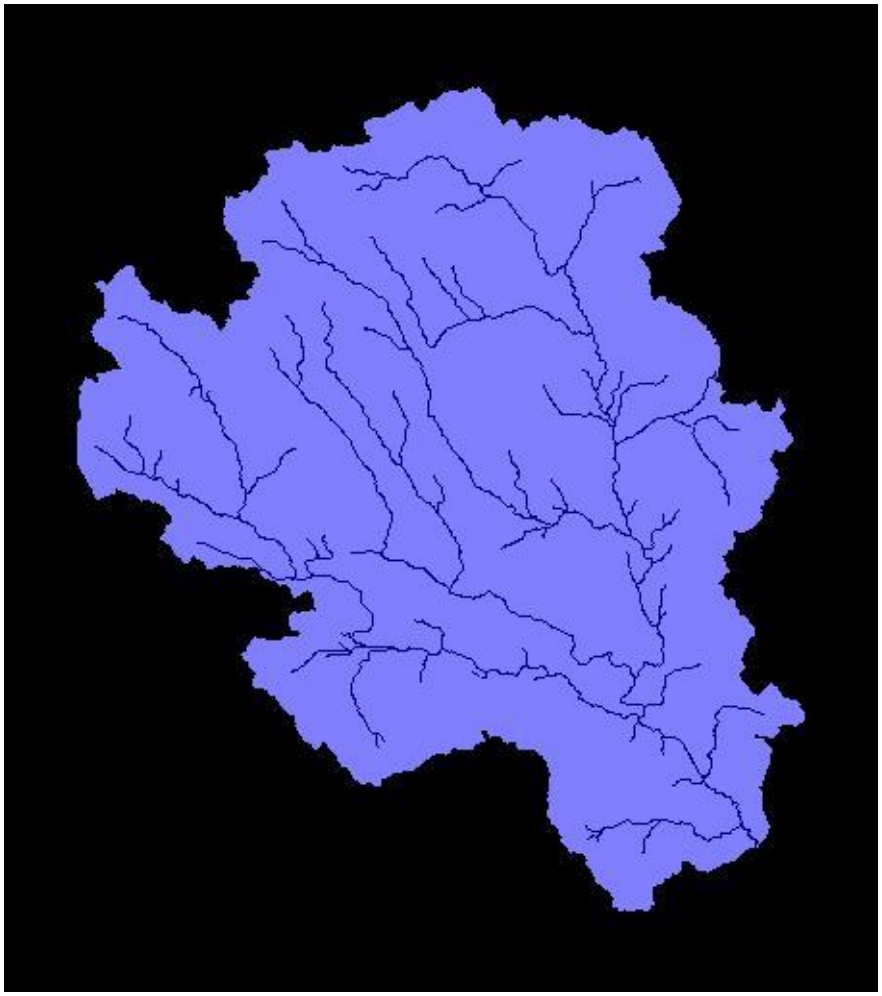

Figure 11: Boundary conditions of the model. Used boundaries: river (blue lines), and recharge (solid light blue)

After successfully defining the property zones, the conceptual model is ready to be assigned a finite difference grid which is the last step before converting the conceptual model into a numerical model. The grid size is an important step in numerical modeling. A coarse grid will run the model quicker but would decrease the accuracy of the results by taking the average of critical attributes, while a finer grid demand longer required computational time to convert and utilize massive computational resources (Wallace, 2016). Considering the impact of numerical grid size on groundwater flow, an optimal grid size (70×70 meter cell size with 163 rows and 144 columns) was selected in study (Marklund & Wörman, 2011) to fulfill multiple grid formations that provides well-accurate results with low conversion time while not consuming a lot of computational resources (figure 12).

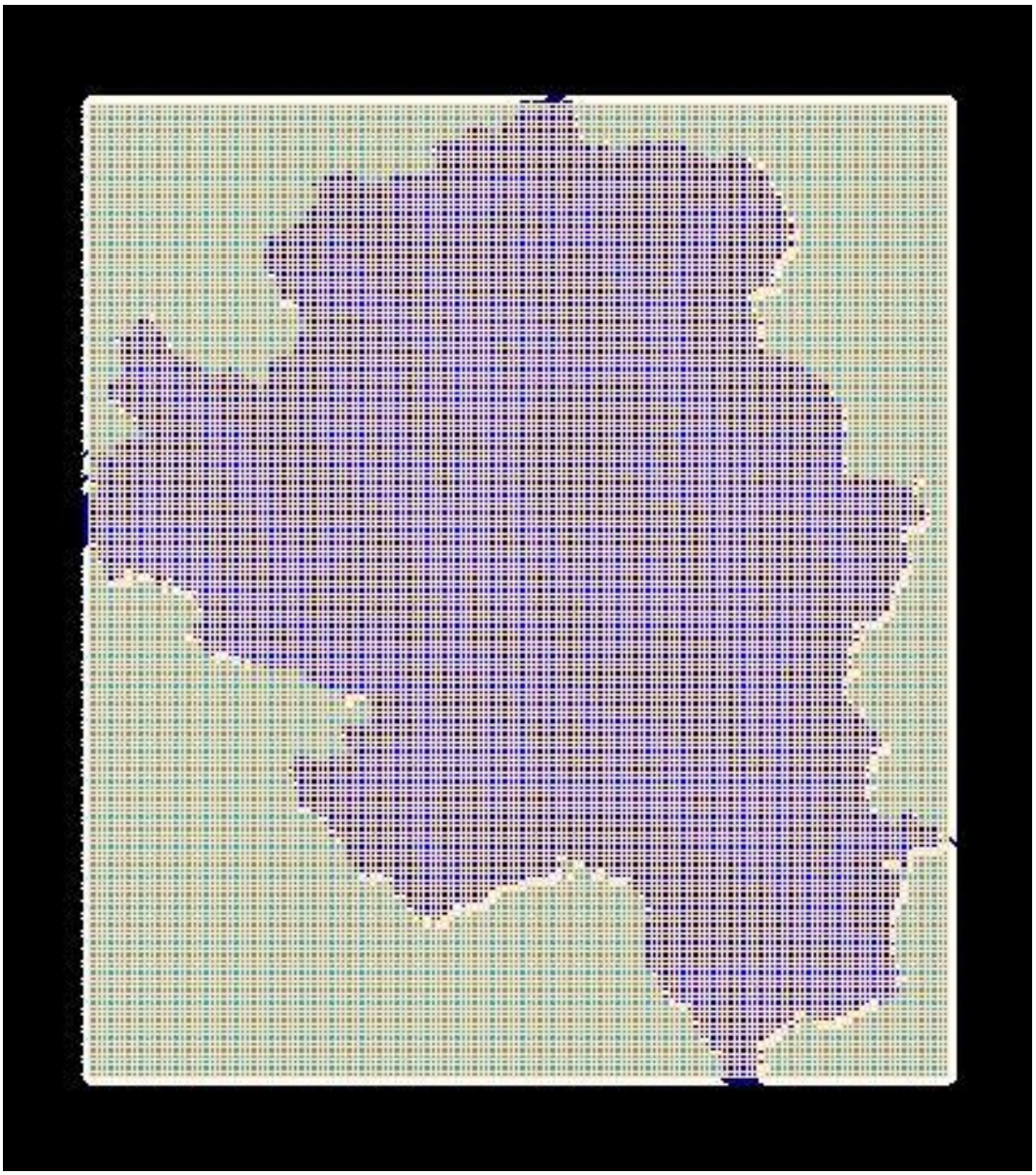

Figure 12: Finite difference grid of the model (70×70m)

3.3.3 Numerical Modeling

Numerical modeling consists of adjusting the boundary conditions, properties of different imported data, running flow engines, and finally analyzing the results. The calibration of the hydraulic conductivities is done at this step after visual evaluation of the simulated model results. The model was run with MODFLOW-2005 engine and PCG solver. The run type was selected at this step of modeling which was performed with a transient run type in this study. The model was run for two time steps on monthly basis which means 12 stress periods (figure 13). This generates results in different categories, e.g. head, water table elevation, velocity etc. with the transient change over a period of one year that was divided into 12 months or stress periods. Figure 14 shows the solver properties used in the numerical modeling. The number of iterations in figure 14

is a parameter that enforces an upper limit on the number of outer and inner iterations that is going to be performed. The designated max number of iterations take place only when a convergent solution is not accomplished beforehand. So, higher number of iterations results in a convergent solution in time.

General

Property Package	**LPF**
Run Type	**Transient**
Steady-State Simulation Time	**1**
Save .FLO file	**Yes**

Property Package

Property Package

Time Steps | Value 1

Stress Period	Start	End	Time Steps	Multiplier
1	0	31	2	1
2	31	59	2	1
3	59	90	2	1
4	90	120	2	1
5	120	151	2	1
6	151	181	2	1
7	181	212	2	1
8	212	243	2	1
9	243	273	2	1
10	273	304	2	1
11	304	334	2	1
12	334	365	2	1

Figure 13: MODFLOW-2005 flow engine settings for the model run

General

Selected Solver	**Conjugate Gradient Solver (PCG)**

PCG2 Settings

Max. outer iteration (MXITER)	**500**
Max. inner iteration (ITER1)	**250**
Pre-conditioning method (NPCOND)	**Modified Incomplete Cholesky (NPCOND=1)**
Head change criterion (HCLOSE)	**0.01**
Residual criterion (RCLOSE)	**864**
Relaxation parameter (RELAX)	**1**
Estimate of the upper bound (NBPOL)	**Calculate esimate**
The printout interval (IPRPCG)	**10**
Convergence output control (MUTPCG)	**Print only the number of iterations(MUTPCG=1)**
Damping factor (DAMP/DUMPPCG)	**1**
Damping factor for transient stress period (DUMPPCGT)	**0.97**

Figure 14: Solver properties used in the model

After assigning the flow engine and solver characteristics, the model was translated and run to attain appropriate results leading to a good analyzation of the model domain and its attributes. It is not usual to be able to achieve the perfect result after the first run, numerical modeling is an iterative process; multiple properties need to be continually modified to come to an acceptable solution.

A particle tracking simulation was also run for 100 particles assigned to each of the river sections to identify the groundwater flow patterns towards the rivers. These particles were propagated backwards in time to track groundwater trajectory path as well as their travel time to reach the stream network from the ground.

4. Results & Discussion

The numerical groundwater model of the Krycklan catchment with river and recharge boundary provided the study with the following results displaying the effect of temporal and spatial differences. Figure 15 represents the monthly recharge rates going into the model.

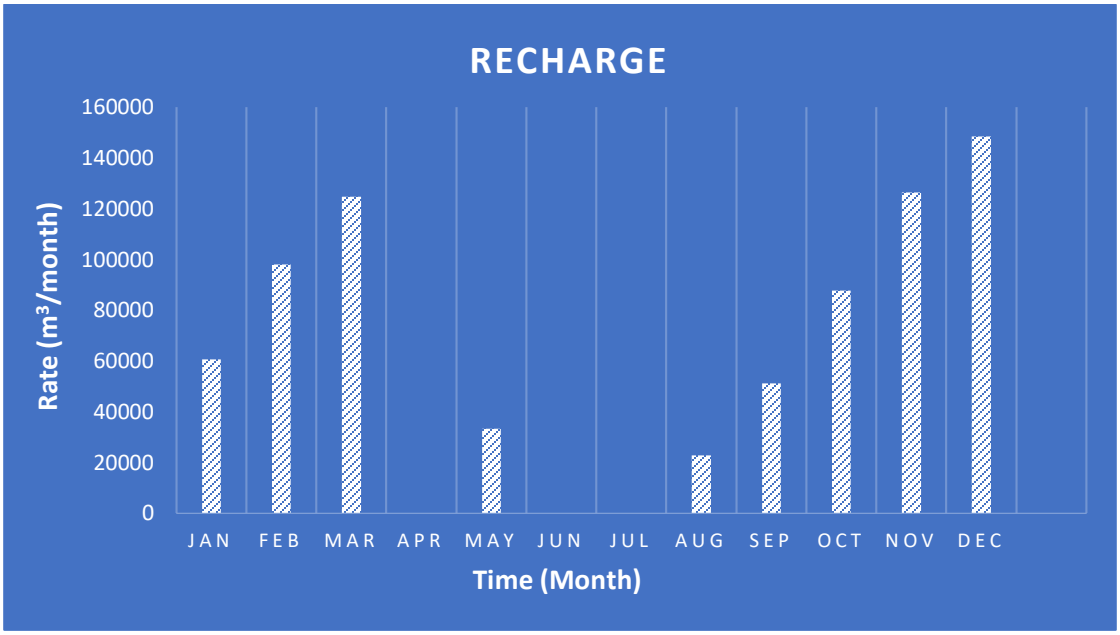

Figure 15: Recharge rate of the model

As it is shown, the rate of the recharge progressively increases from January-March and then suddenly hits zero in April. This is because the model does not consider any negative recharge into the system. During April, June, and July, the rate of evapotranspiration was higher than the amount of precipitation received by the catchment (table 3), which ultimately resulted in a negative or zero recharge. This decline in recharge is followed by a rising recharge rate from August-December with the highest recharge rate (148,414 m^3/month) monitored in December. Now, as the precipitation data considers both snowfall and rain, the recharge rates are acceptable.

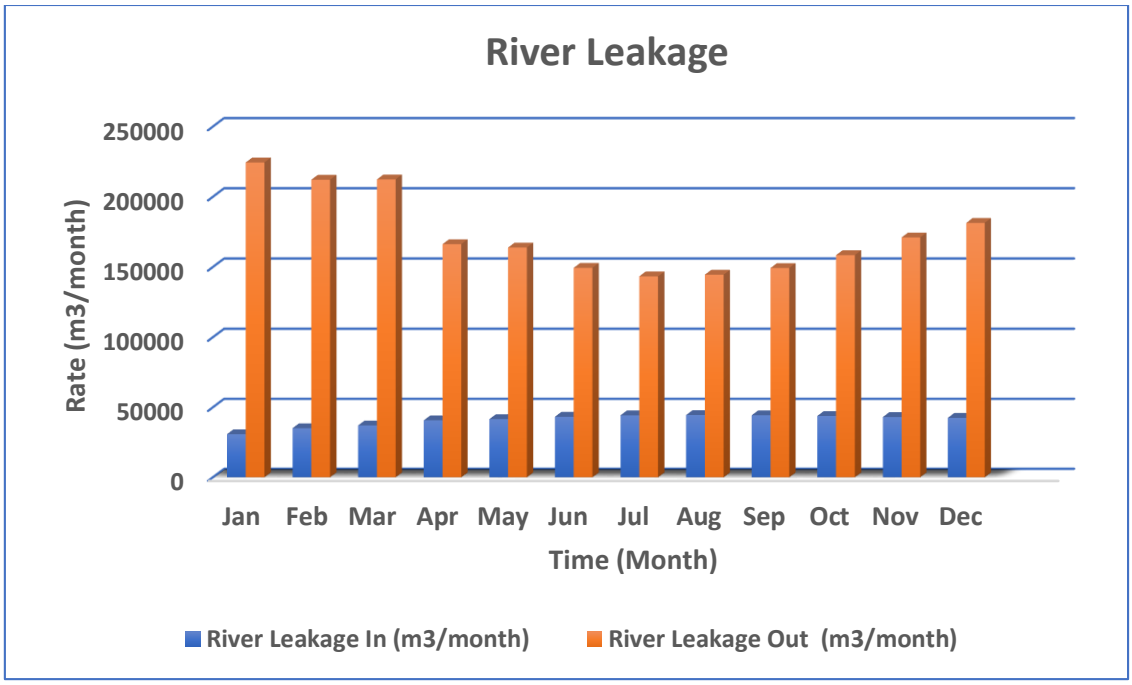

Figure 16: River Leakage rate of the model

There is a relation between surface water bodies such as- rivers, streams, and lakes, and the groundwater which are influencing each other (Boano et al., 2014; Lewandowski et al., 2019). Depending on the difference of hydraulic gradient between the groundwater system and the surface water bodies, the groundwater system might seep into the river or the river might behave as a groundwater discharge zone, and it is important for a groundwater model to simulate those relations into the model to make it even more precise.

The river leakage rate is a very efficient way to know how much water has traveled back and forth between the river and the groundwater and for this model, it is calculated by Visual MDFFLOW Flex 6.1 from the provided data in table 1. The 'river leakage in' indicates the amount of water that has come into the river body (source) from the groundwater system, while the 'river leakage out' indicated the water that has leaked from the river through the riverbed into the groundwater system. In figure 16, it is observed that the rivers in Krycklan are contributing to the groundwater system (sink) by a volumetric flow rate of at least 143,000 m^3/month while getting approximately 35,000 m^3/month as 'river leakage in' from the groundwater system throughout the year.

Questions might arise as to why the river leakage in and out are not equal through the year, this is due to the fact that it is one of the components for the calculation of the total inflow and outflow of the whole system. The equation solving system of a model requires a flow continuity statement for each model cell i.e. a continuity must exist for the total flows of the model (MODFLOW 6-Description of Input and Output, 2017).The model takes the recharge in consideration, calculates the river leakage with equation 6, and also calculates the storage values and then determines the entire model's total flow (figure 18) that shows almost equal inflow and outflow through the year which validates the model's acceptability.

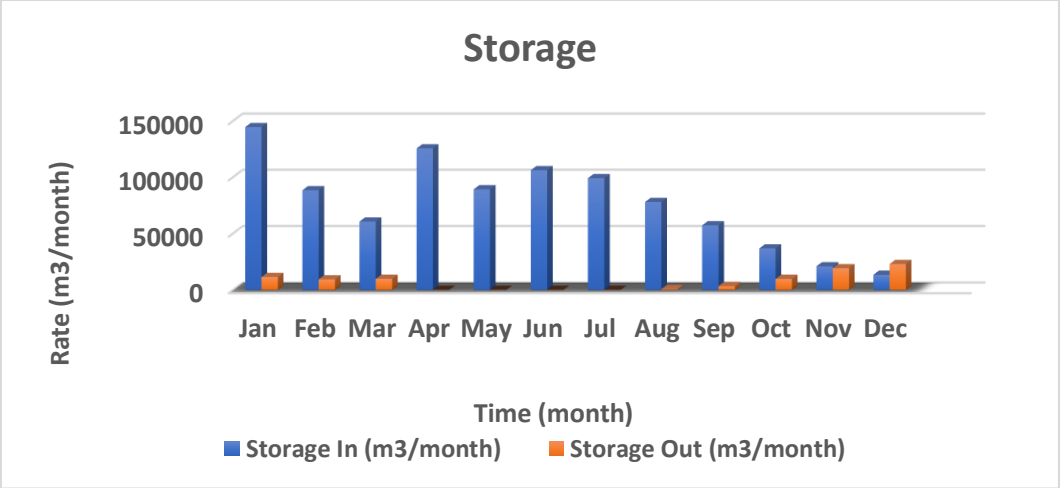

Figure 17: Storage rate of the model

Figure 17 illustrates the groundwater storage simulated by the model from the provided recharge and river data as well as river and recharge boundary conditions for the Krycklan catchment. It shows the highest storage rate in January with a value of 140,000 m3/month and the lowest in December with a value of 13,000 m3/month only. The varying volumetric storage rates are of course an interpretation of the variable recharge input and the constant stream data but there are other factors to be considered as well. According to Jutebring Sterte, et al., (2018), the groundwater flow variability can be explained by the difference in the catchment characteristics e.g. soil properties and freeze-thaw processes during different time of the year. The graph shows that the rate of storage going out of the groundwater system is very low considering the rate of storage going in through the year. This information might be useful for possible groundwater extraction scenario if needed in the future provided a safe yield approach is taken into consideration.

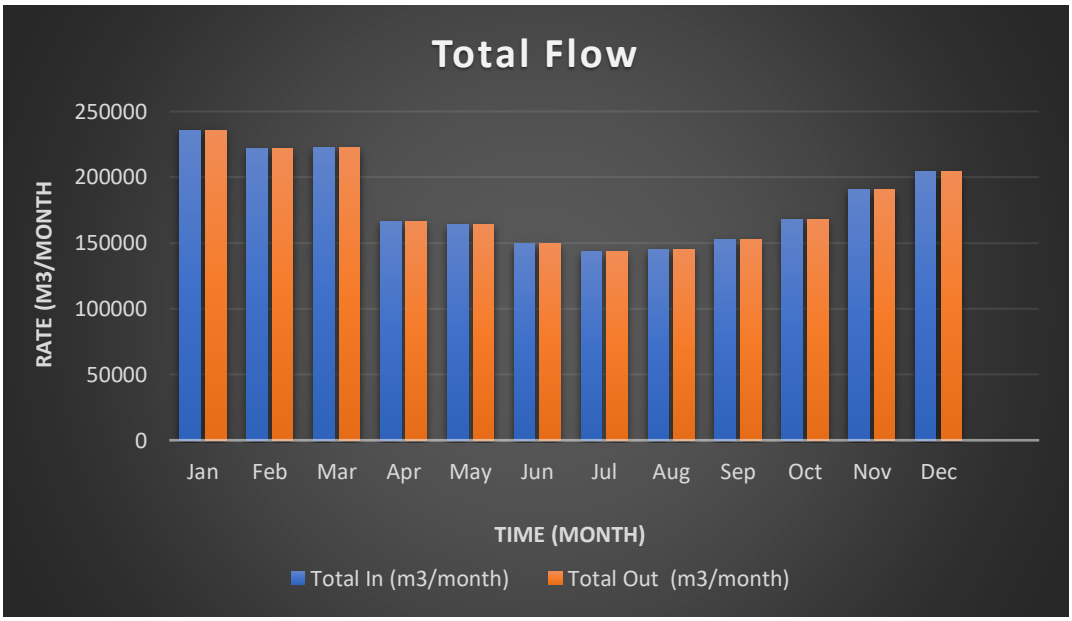

Figure 18: Total flow of the model

There should not be too much of a difference between the total inflow and total outflow of a well-designed and balanced system. A lower percent discrepancy in the model total flow rates promotes more accuracy of the solved model equations (MODFLOW 6- Description of Input and Output, 2017). Figure 19 highlighted the difference between total inflow and outflow for Krycklan catchment which is almost indistinguishable for the entire year. The total flow is the highest in January for the catchment while the lowest is in July. When looked carefully, it can be noticed that the graph pattern for figure 18 is similar to figure 16 as the river leakage out rate of figure 16 is contributing significantly to the total outflow rate of the system.

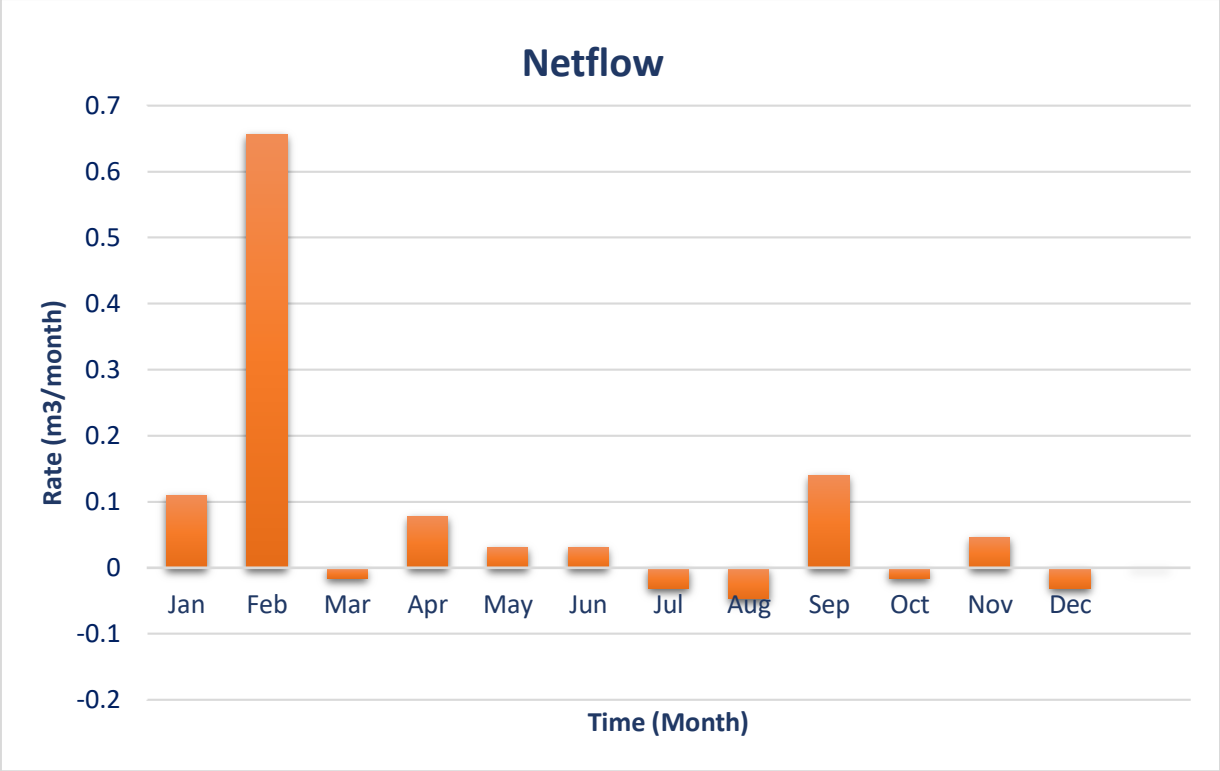

Figure 19: Netflow of the model

The temporal change in the flow mass balance (i.e. the difference between the total inflow and the total outflow or known as netflow) can be very helpful to understand the dynamics of the groundwater system of a model. Figure 19 demonstrates the netflow rate over a year for each month. It indicates the highest netflow rate (0.65 m^3/month) in February, meaning that the total inflow was the higher than the total outflow by 0.65 m^3/month.

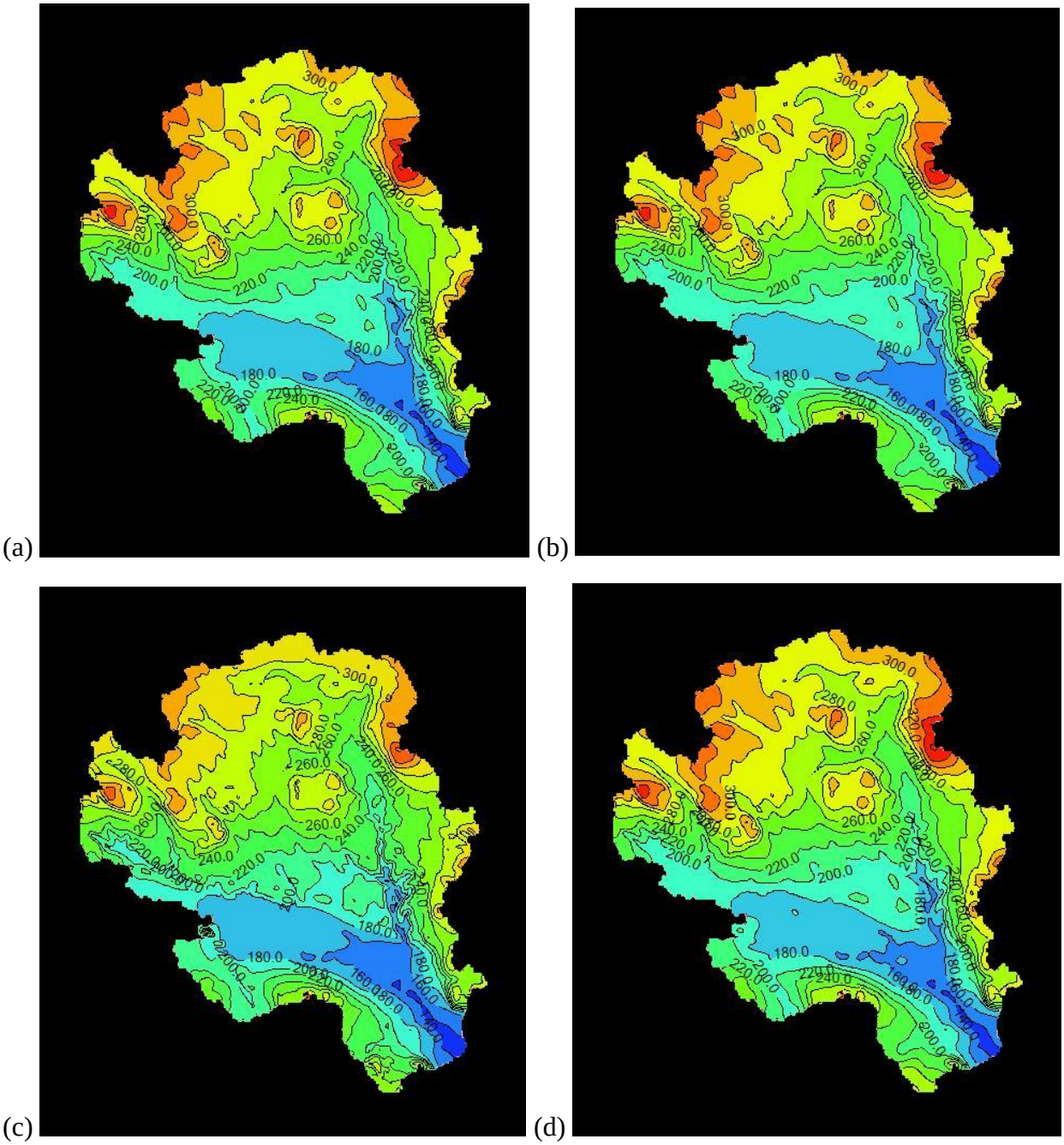

Figure 20: Water table elevations of the model in (a) summer (Jun), (b) fall (Aug), (c) winter (Nov), and (d) spring (Apr)

Figure 20 illustrates the temporal change in water table elevation within the catchment for each season. In figure 20 (a) the beginning of the summer is portrayed, there are moderately high water table elevations (300m) around the north-east and most of the north-west corner of the model domain. There are mostly peat and bedrock outcrops with some fracture zones in that region of the catchment. The elevations in the downstream part of the catchment are higher near the edges which gradually lowers down in the middle part with the lowest elevation of 140m in the stream. In figure 20 (b) or in the beginning of fall, no significant difference in elevation was observed in the

catchment from the summertime. This is because the model rarely got any recharge during summer and fall (figure 15). More area with higher elevations of the water table were observed during winter with 300 m in most of the northern boundary of the catchment which gradually decreases by 20 m (similar to summer and fall but with more contour levels) while coming downstream. Since water table elevations vary with temporal changes (seasonal change) as well as due to spatial change (surface elevation), it is quite typical to find higher water elevations in winter-upstream of Krycklan as it receives the most infiltration during winter (table 3). During spring (figure 20(d)), the water table almost declines back to the summer elevations but still had more areas with higher elevations than summer as there were higher amount of infiltration during those months. There are maps of the water table elevation for all the months presented in figure A-2 attached in the appendix.

Backward particle tracking (figure 21) was also done on the model to identify how groundwater is moving towards the streams which results in a high river leakage out. 100 particles were assigned evenly on each of the stream groups at the topography surface in order to track the travel time taken for the groundwater to reach those stream group as well as to see the trajectory of the groundwater flow.

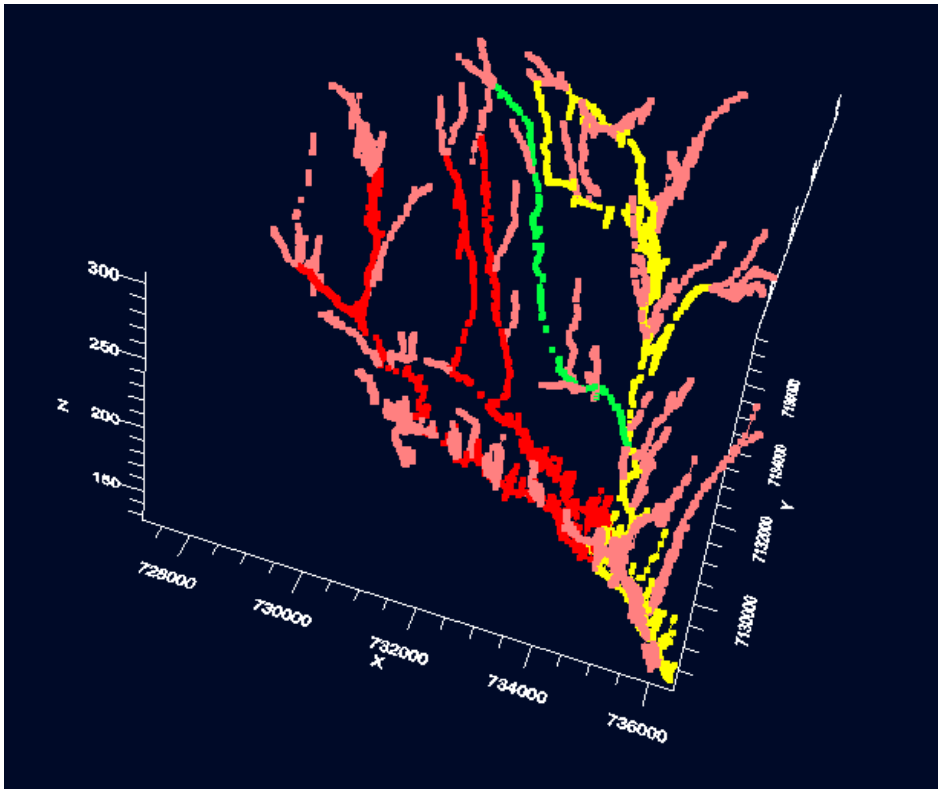

Figure 21: 3D view of the particle tracking of river sections

Figure A-3 exemplifies a zoomed version of figure 21, which helps to clearly see the pathlines with the time intervals represented as nodes on the pathlines. The yellow, green, red, and pink color correspond to the river group 1, 2, 3, and 4, respectively in figure 21.

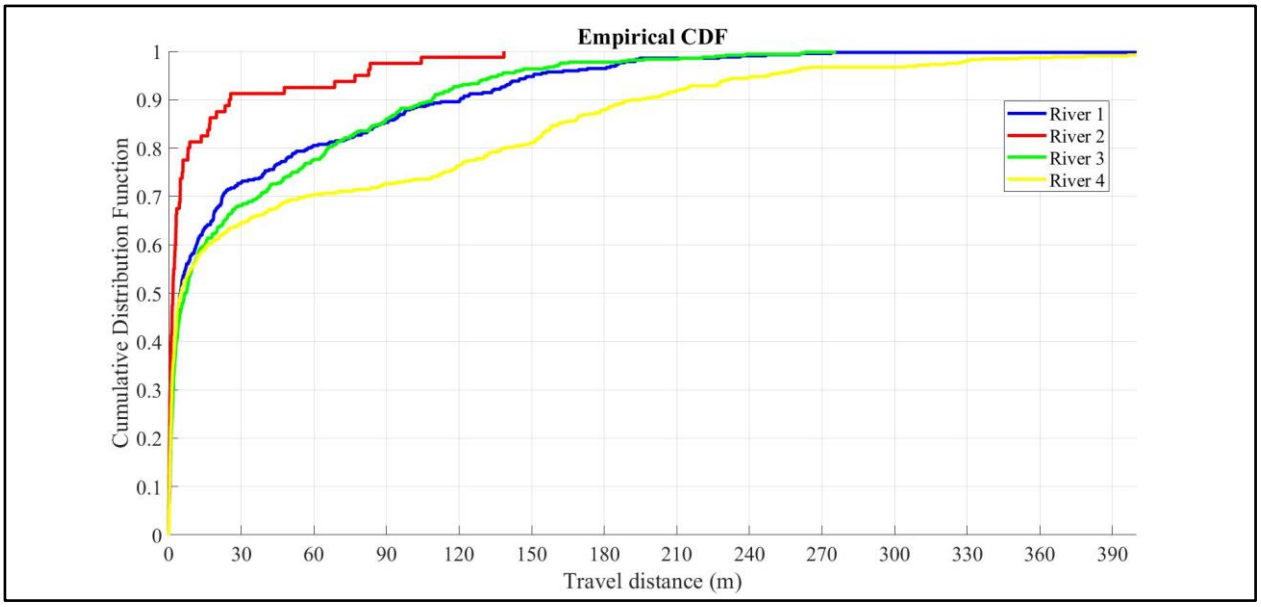

Figure 22: A CDF chart of the travel distance by the river particles

Figure 22 and 23 are fine depiction of the travel distance and travel time of the river particles. The Cumulative Distribution Function (CDF) plots are created in MATLAB. Figure 22 shows that for stream group 1 and 3, particles travel almost the same amount of distance; 80% of these river particles travel a same distance of 70m. 80% of group 2 particles only travel a distance of 15m, that shows a shallow pathline of particles. The longest distance traveled are by the group 4 particles at a distance of 380m; 80% of its particles traveled a distance of 140m, which means the stream tributaries are in a deeper contact with the groundwater flow than the other river sections.

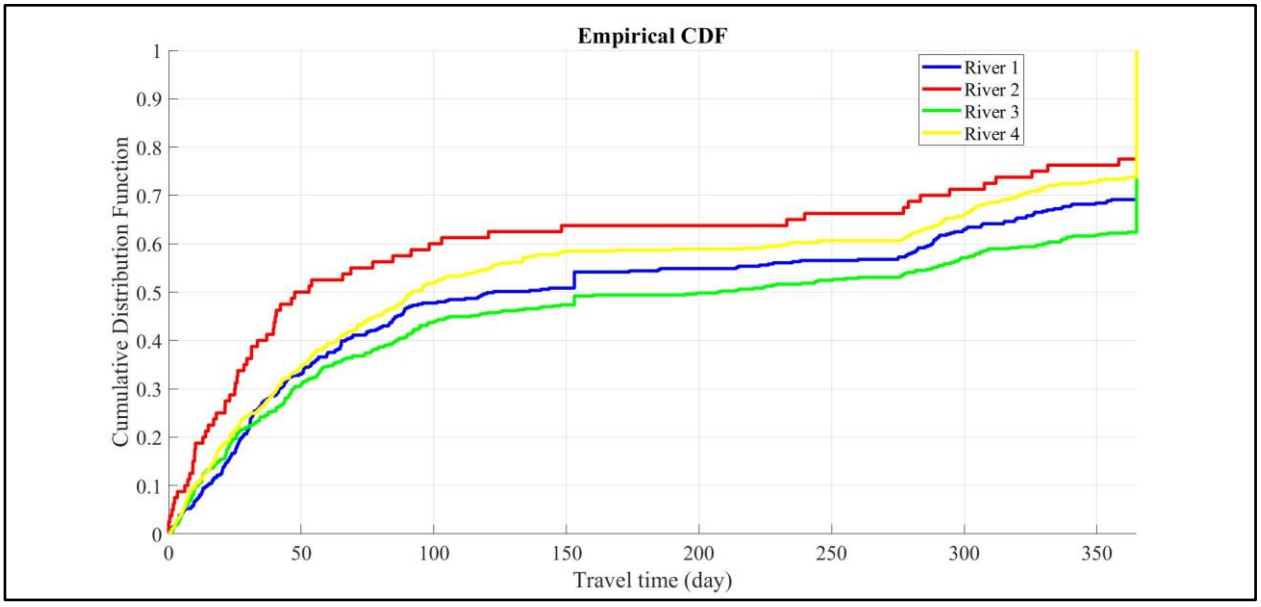

Figure 23: A CDF chart of the travel time by the river particles

Now, figure 23 portrays the travel time for these river particles and presents how long it might take for the river particles to travel their pathlines. All of the river particles seem to follow a similar curve in the travel time CDF plot, where the group 2 particles were found to be the fastest with 60% of the particles travelling to the end of pathline in 100 days when it takes the same amount of days for 52%, 48%, and 44% of the group 4, 1, and 3 particles to reach the end of their pathlines, respectively. A noticeable change is observed at the end of figure 25, where all the river particles suddenly reaches completion. This is because these particles have been tracked for a maximum of 365 days. Hence, it is concluded that the particles need more time to finish reaching the end of their pathlines.

5. Conclusion

The key objective of this study was to attain a better knowledge of the temporal impacts of the climate condition on the groundwater flow of the Krycklan catchment with a numerical transient modelling approach. The study found the following limitations while accomplishing this objective, which could be improved for a better model.

Firstly, grid size in any numerical modelling is one of the most important elements to think profusely about. If a model grid size is too coarse, the final numerical grid of the model would not be able to accomplish being a good representation of the real characteristics of the actual study area. It would make slopes steeper in an effort to force a bigger area fit into one small grid. It might also overlap the attributes of soil types situated close to each other that results in false or unnatural results after the model run. Again, a model that has a finer grid size would be able to depict the natural physical attributes of the study area, leaving a smaller area for error, providing the input data and boundary conditions are correct, it would take much more time and resource to convert and run. Finding the perfect grid size also depends on the size of the area to be modeled.

This study finally used a 70 m grid size after attempting to model the Krycklan catchment with 500 m, 200 m, 100 m, 70 m, and 50 m grid sizes. The models created with more than a 100m grid size were too coarse to capture the reality of the catchment. The groundwater flow intensity appeared to be more similar to the actual situation after decreasing the grid size from 100 m to 70 m. An effort was taken to make the grid size even smaller, to achieve an improved representation of the topography but was later discarded as it took a lot of time and resources to process.

Secondly, the study is supposed to be done in a transient state with transient data, but it was not possible as there was a lack of temporal changes of river cross-section information of the catchment rivers. The river width of the catchment's rivers varies from 0.5 m-4.78 m according to the collected data, but this data cannot be constant through every season or month of the year. New studies should be carried out on the temporal and spatial changes of the river cross-sections of the catchment to obtain a more accurate numerical groundwater model of the catchment.

Thirdly, the number of variables that are used in a study certainly affects the precision of the results. The variables put in this study are the monthly recharge data, hydraulic conductivity, and the river data, but in order to obtain more accurate knowledge of the groundwater flow of the

catchment and to increase the model validity, more information, e.g. storativity of the soil types, observed well data, pumping well data, discharge data etc. should be included in the model.

From the results of the numerical transient modelling, the study found the following temporal impacts of the climate condition on the groundwater flow of the Krycklan catchment.

A mass balance of the river leakage was expressed in a graph varying in time. The higher rate of "river leakage out" than "river leakage in" at each time interval suggested that there might be an active leakage of surface water into the groundwater going on in the catchment groundwater flow system. The amount of water going into the groundwater from the rivers is the highest in January (220,000 m3/month) while maintaining an inflow of at least 143,000 m3/month. This inflow follows a steady concave down, decreasing curve from January-May, and then follows a concave up, increasing curve from June-December. Also, when accounting for the particle tracking of the river particles, the contribution of each stream group to the river leakage graph of the model area can be easily observed. The stream tributaries seem to have a deeper and faster connection to groundwater than the other stream groups although, group 1 and 3 also have significantly fast travel time and long travel distance which shows a relatively good interaction with groundwater with the flow of time. Similar to the river leakage results, the mass balance of the total flow of the system is also seen to follow identical curves around the year.

Variations have been observed in the water table elevation in different areas of the catchment at different times of the year. These changes are directly impacted by the daily precipitation and evapotranspiration data as well as the hydraulic conductivity of the soil types. The maximum water table elevations noticed in all seasons are on the north and upstream region of the catchment which agrees with the topography of the catchment.

Finally, even with the discussed limitations, the model is helping to take a step forward in understanding the concept of groundwater flow and the how it is impacted with the change in time of the Krycklan catchment area. The whole process starting from data collection to building a groundwater model from scratch has been very educational. It provided an in-depth knowledge of the natural systems that becomes clearer with more modelling work. In order to attain an even more deep understanding of the study area and its natural processes with more precise and newer information, this model should act as a steppingstone for future modelers.

6. Reference

Ahsan, N. U. (2019). Assessment of saltwater intrusion in the south western coastal aquifers of Khulna using Visual MODFLOW.

Allen, R. G., Pereira, L. S., Raes, D., Smith, M. (1998). *Crop evapotranspiration - Guidelines for computing crop water requirements - FAO Irrigation and drainage paper 56*. Rome: Food and Agriculture Organization of the United Nations.

Anderson, M. P., Woessner, W. W. & Hunt, R. J. (2015). *Applied Groundwater Modelling*. Cambridge: Academic Press.

Baalousha, H. (2008). *Fundamentals of Groundwater Modelling*. Napier: Nova Science Publisher.

Boano, F., Harvey, J. W., Marion, A., Packman, A. I., Revelli, R., Ridolfi, L., & Wörman, A. (2014). Hyporheic flow and transport processes: Mechanisms, models, and biogeochemical implications. Reviews of Geophysics, 52(4), 603-679.

Bredehoeft, J.D., and Hall, P. (1995*). Ground-water models; Groundwater, v. 33*

Chen, Z., Grasby, S.E. and Osadetz, K.G., 2002. Predicting average annual groundwater levels from climatic variables: an empirical model. *Journal of Hydrology*, *260*(1-4), pp.102-117.

Chow, V. T., Maidment, D. R., & Mays, L. W. (1988). *Applied hydrology*. New York: McGraw-Hill.

Gomez Peña, C. A. (2017). Simulation and Prediction of the Groundwater Level in the Surrounding Area of the Nebraska Management System Evaluation Area site in Central Nebraska.

Harbaugh, A.W. (2005). MODFLOW-2005, the U.S. Geological Survey modular ground-water model - the Ground-Water Flow Process: U.S. Geological Survey Techniques and Methods 6-A16. This report describes the theory and input instructions at the time of the initial MODFLOW-2005 v1.00 release.

Hill, Mary. (2006). The practical use of simplicity in developing groundwater models. *Ground water Journal, 44(6)*: 775-781

Jaremalm, M., & Nolin, L. (2006). Survey of the riparian zone along streams in Krycklan. Unpublished field report. 51p.

Jin-sheng, Jia, Jing-jie, Yu,Chang-ming, Liu (2002). Groundwater regime and calculation of yield response in North China Plain: a case study of Luancheng County in Hebei Province. Water Resources, *Journal of Geographical Sciences*.

Jutebring Sterte, E. (2016. Integrated hydrologic flow characterization of the Krycklan catchment (Sweden).

Jutebring Sterte, E., Johansson, E., Sjöberg, Y., Karlsen, R.H., Laudon, H., 2018. Groundwater-surfacce water interactions across scales in a boreal landscape investigated using a numerical modelling approach. *Journal of Hydrology*, Volume 560, pp. 184-201.

Jyrkama, M.I. and Sykes, J.F., 2007. The impact of climate change on spatially varying groundwater recharge in the grand river watershed (Ontario). *Journal of Hydrology*, *338*(3-4), pp.237-250.

Laudon, H., Taberman, I., Ågren, A., Futter, M., Ottosson-Löfvenius, M., & Bishop, K. (2013). The Krycklan Catchment Study—A flagship infrastructure for hydrology, biogeochemistry, and climate research in the boreal landscape. *Water Resources Research*, *49*(10), 7154-7158.

Lekula, M., Lubczynski, M. and Shemang, E. (2018). Hydrogeological conceptual model of large and complex sedimentary aquifer systems – Central Kalahari Basin (Botswana). Physics and Chemistry of the Earth, Parts A/B/C.

Lewandowski, J., Arnon, S., Banks, E., Batelaan, O., Betterle, A., Broecker, T., ... & Gomez-Velez, J. (2019). Is the hyporheic zone relevant beyond the scientific community? *Water*, *11*(11), 2230.

Marklund, L., & Wörman, A. (2011). The use of spectral analysis-based exact solutions to characterize topography-controlled groundwater flow. *Hydrogeology Journal*, *19*(8), 1531-1543.

McCuen, R.H., 2016. *Modeling hydrologic change: statistical methods*. CRC press.

Mojarrad, B. B., Riml, J., Wörman, A., & Laudon, H. (2019). Fragmentation of the hyporheic zone due to regional groundwater circulation. *Water Resources Research, 55, 1242– 1262*. https://doi.org/10.1029/2018WR024609

Mojarrad, B. B., Betterle, A., Singh, T., Olid, C., & Wörman, A. (2019a). The effect of stream discharge on hyporheic exchange. *Water*, *11*(7), 1436.

Morén, I., Wörman, A., & Riml, J. (2017). Design of remediation actions for nutrient mitigation in the hyporheic zone. *Water resources research*, *53*(11), 8872-8899.

Scibek, J., Allen, D.M., Cannon, A.J. and Whitfield, P.H., 2007. Groundwater–surface water interaction under scenarios of climate change using a high-resolution transient groundwater model. *Journal of Hydrology*, *333*(2-4), pp.165-181.

Vijay P. Singh, Ph.D., D.Sc., D. Eng. (Hon.), Ph.D. (Hon.), D. Sc. (Hon.), P.E., P.H., Hon. D. WRE, Academician (GFA*). Handbook of Applied Hydrology*, Second Edition. HYDROLOGIC CYCLE, Chapter (McGraw-Hill Education: New York, Chicago, San Francisco, Athens, London, Madrid, Mexico City, Milan, New Delhi, Singapore, Sydney, Toronto, 2017).

Wallace, B. M. (2016). NCMA groundwater model using USGS MODFLOW-2005/PEST.

Wu, Y., Liu, S. and Gallant, A.L., 2012. Predicting impacts of increased CO2 and climate change on the water cycle and water quality in the semiarid James River Basin of the Midwestern USA. *Science of the Total Environment, 430*, pp.150-160.

Other sources

Darwin, C. 2010, Climate Change and Groundwater

Groundwater flow. Viewed 13 March 2020, https://en.wikipedia.org/wiki/Groundwater_flow

Groundwater flow equation. Viewed 13 March 2020, https://en.wikipedia.org/wiki/Groundwater_flow_equation

Hydrological Research at Krycklan Catchment Study, Viewed 19 February 2020, https://www.slu.se/en/departments/field-based-forest-research/experimental-forests/vindeln-experimental-forests/krycklan/

Laudon, H 2017, The Krycklan Catchment Study -A unique infrastructure for field based research on hydrology, ecology and biogeochemistry, Viewed 2 March 2020, https://www.slu.se/en/departments/field-based-forest-research/experimental-forests/vindeln-experimental-forests/krycklan/infrastructure/

MODFLOW 6 – Description of Input and Output, USGS , Version mf6.0.0 – August 11, 2017 https://water.usgs.gov/ogw/modflow/mf6io.pdf

Precipitation. Viewed 02 March 2020, https://en.wikipedia.org/wiki/Precipitation

©Sveriges geologiska undersökning (SGU), Viewed 17 February 2020, https://apps.sgu.se/kartvisare/kartvisare-jordarter-25-100.html?zoom=98683.01761803502,6875669.98144996,1054884.9300218602,7313170.856451711

The Krycklan Infrastructure 2020, Viewed 15 March 2020, https://www.slu.se/en/departments/field-based-forest-research/experimental-forests/vindeln-experimental-forests/krycklan/infrastructure/

USGS, 1984, *The Hydrologic Cycle*, USA

Visual MODFLOW Flex. Viewed 20 March 2020, https://www.waterloohydrogeologic.com/visual-modflow-flex/

Visual MODFLOW Flex 6.1 Integrated Conceptual & Numerical Groundwater Modeling Software, User's Manual, Waterloo Hydrogeologic, Waterloo, Canada, 2019. https://www.waterloohydrogeologic.com/help/vmod-flex/hmcontent.htm

What is climate change?, Viewed 02 March 2020, https://climatekids.nasa.gov/climate-change-meaning/

Appendix

Table A-1: River section details

River section in model	Number of measured cross section	Secton in report	River Width- Median B (cm)	River Depth- Median E (cm)	weigthed avg Width (cm)	weigthed avg Depth (cm)	Considered Width (cm)	Considered Depth of water (cm)
1	6	L	420	28	478.1818	30.90909	**478**	**31**
	16	M	500	32				
2	12	I	94	26	103.36	29.12	**103**	**29**
	13	J	112	32				
3	12	A	67	20	86.08333	24.31373	**86**	**24**
	7	B	135	20				
	18	D	84	23				
	9	E	84	20				
	14	F	82	19				
details	12	G	42	15	53.16216	10.7027	**53**	**11**
	11	H	49	12				
	14	K	66	6				

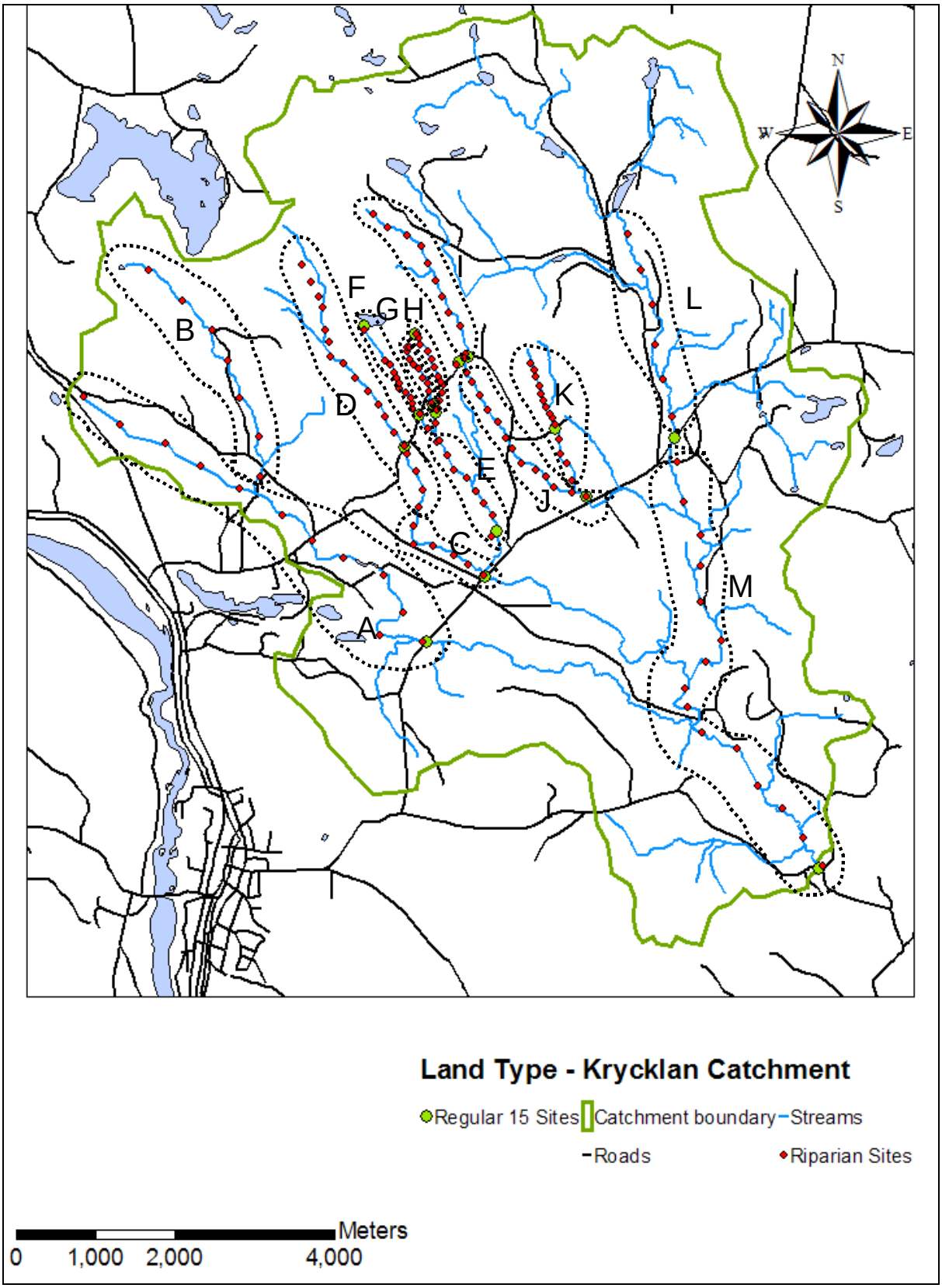

Figure A-1: KCS area with river sections shown in dotted lines

A.

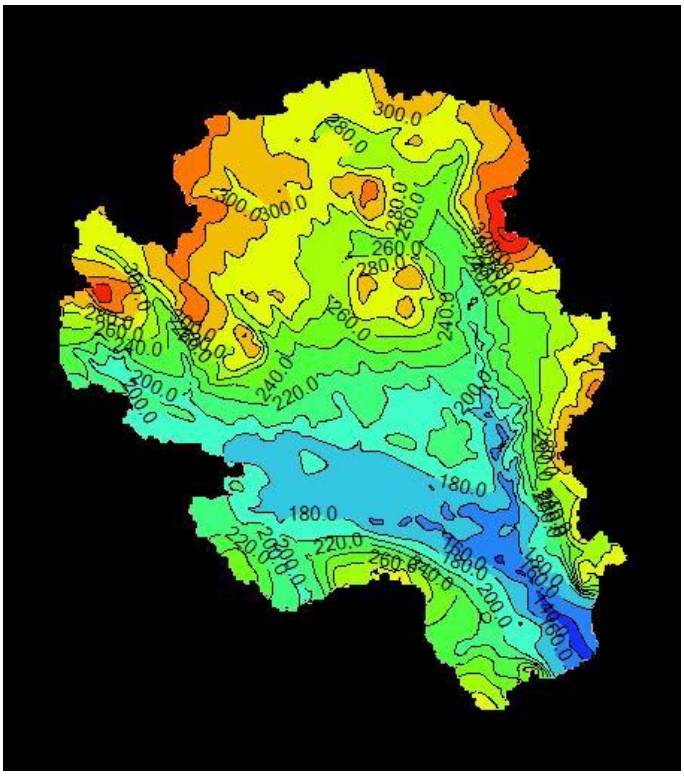
300.0
280.0
260.0
240.0
220.0
200.0
180.0
160.0

B.

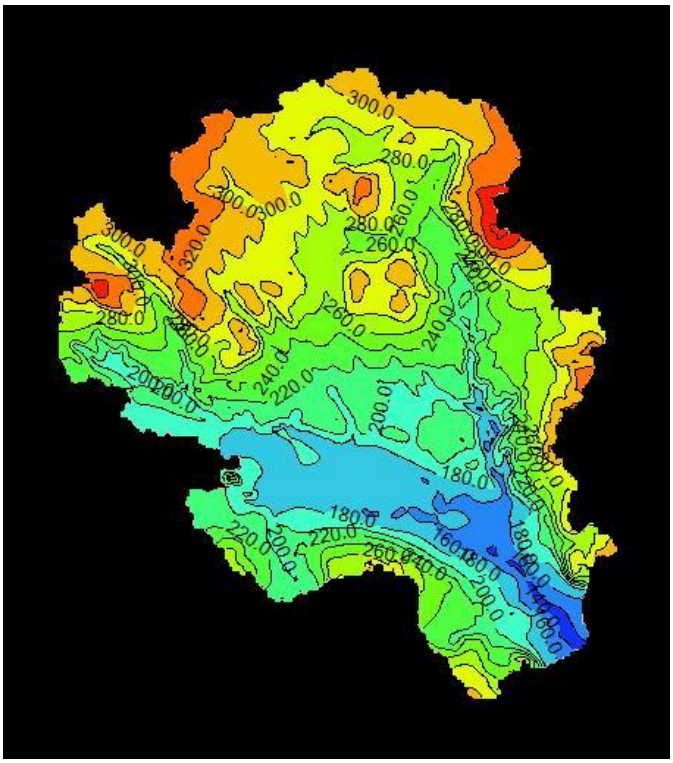
300.0
280.0
260.0
240.0
220.0
200.0
180.0
160.0

C. 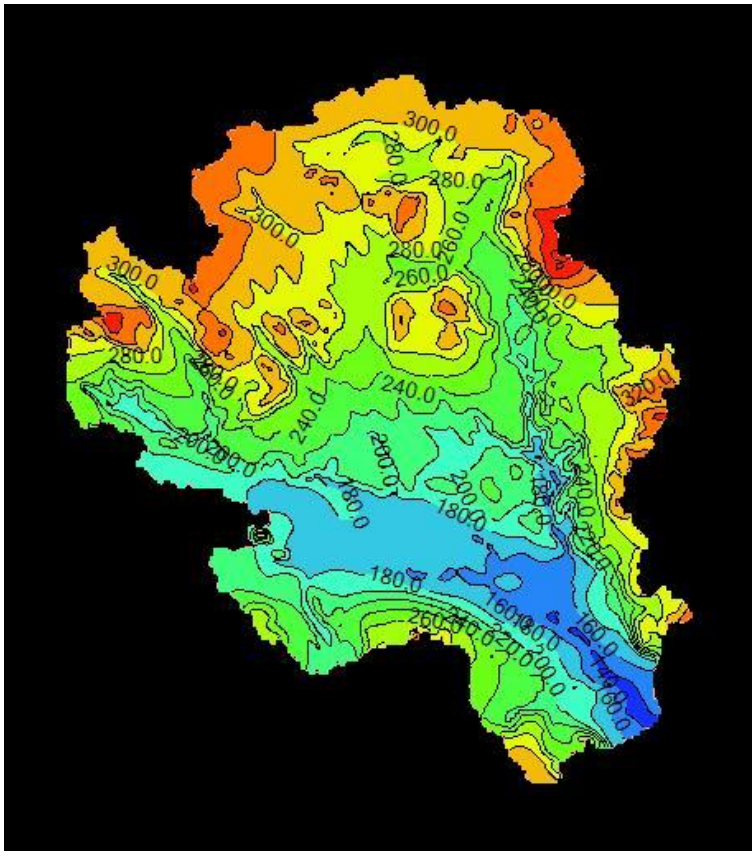
300.0
280.0
260.0
240.0
220.0
200.0
180.0
160.0

D. 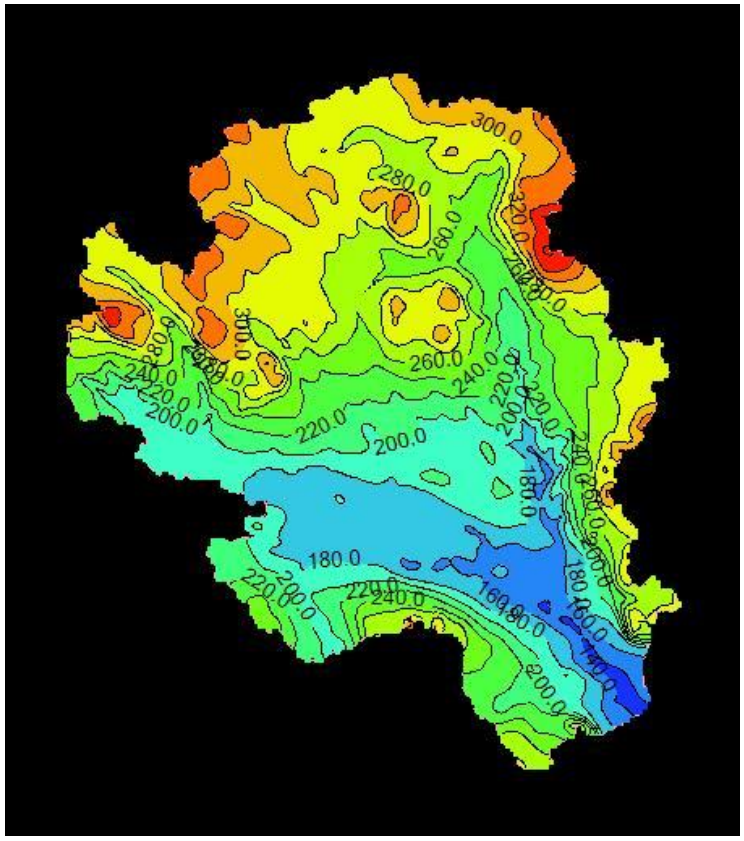
300.0
280.0
260.0
240.0
220.0
200.0
180.0
160.0

E.

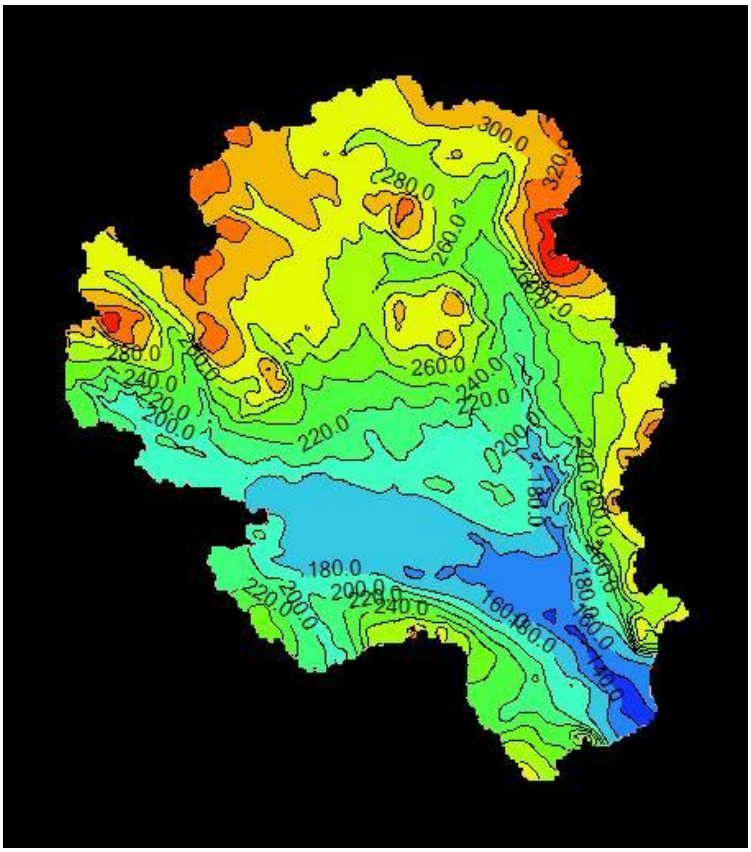
300.0
280.0
260.0
240.0
220.0
200.0
180.0
160.0

F.

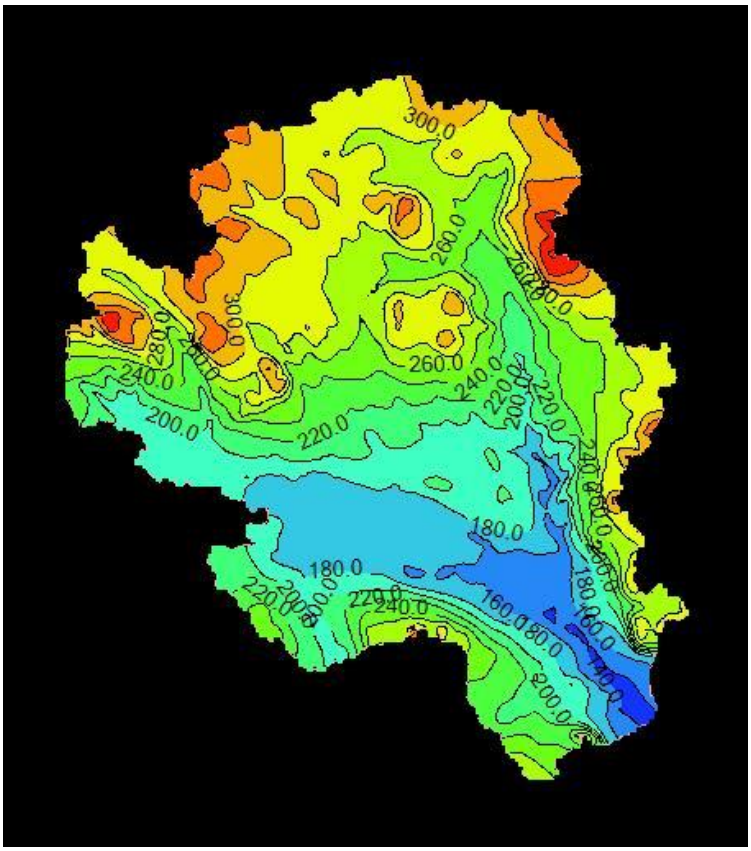
300.0
280.0
260.0
240.0
220.0
200.0
180.0
160.0

G. 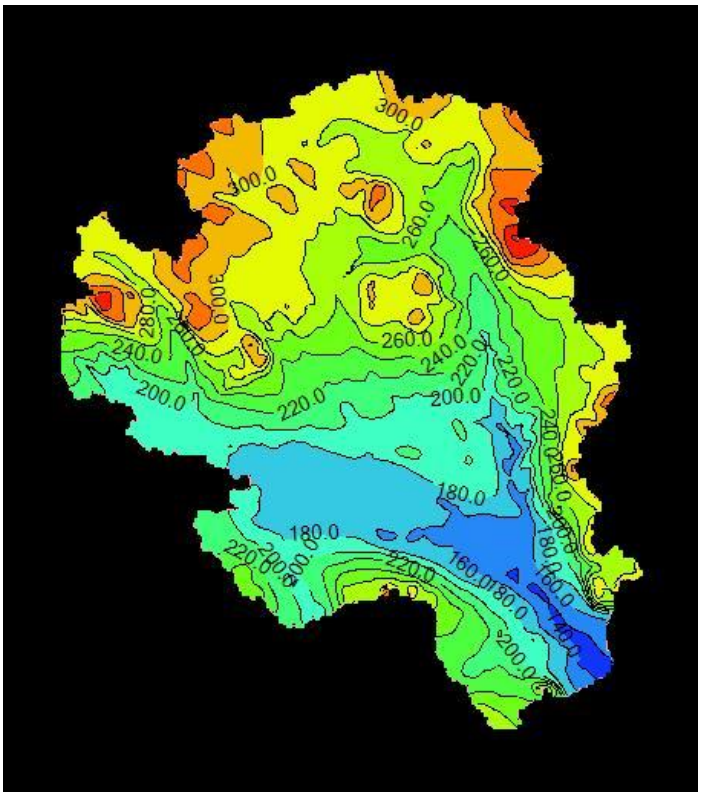
300.0
300.0
280.0
260.0
300.0
280.0
240.0
260.0
240.0
220.0
220.0
200.0
200.0
220.0
180.0
180.0
220.0
160.0
180.0
200.0

H. 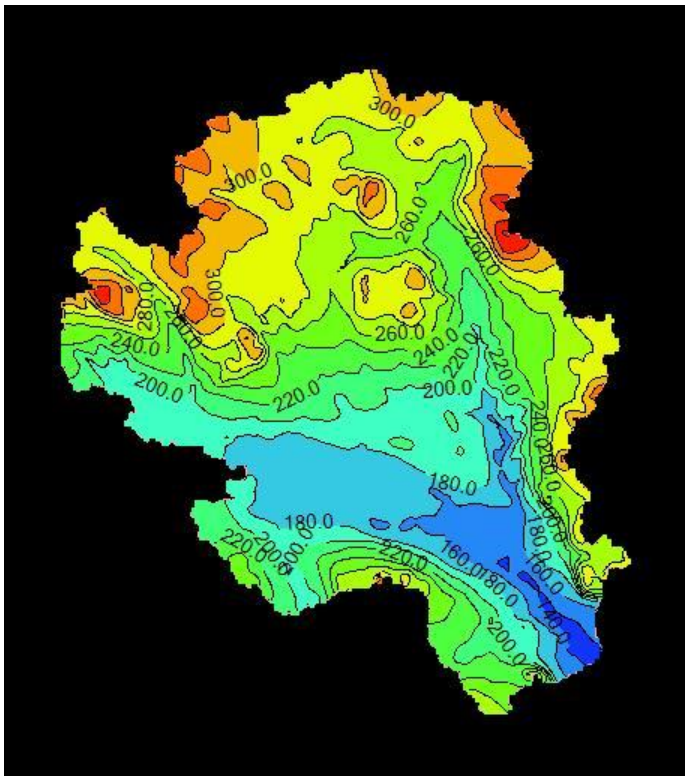
300.0
300.0
280.0
260.0
300.0
280.0
240.0
260.0
240.0
220.0
220.0
200.0
200.0
220.0
180.0
180.0
220.0
160.0
180.0
200.0

I.

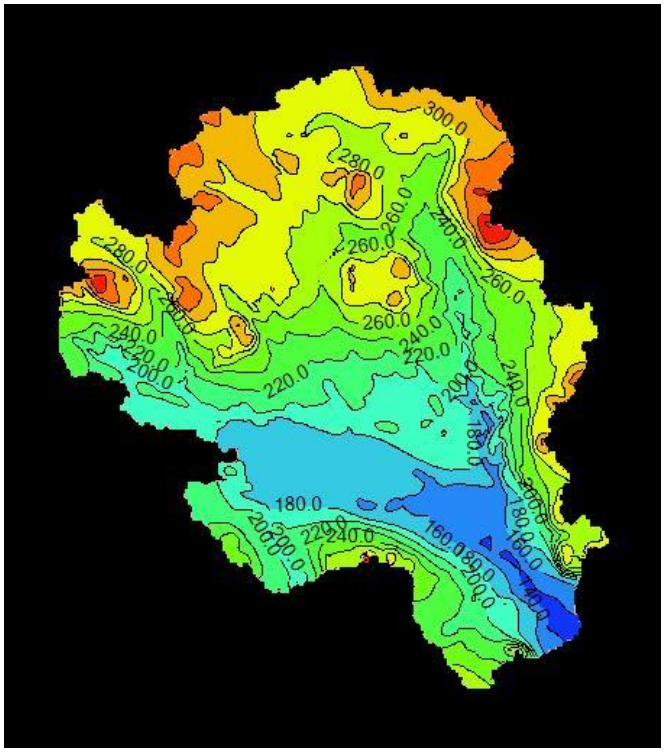
300.0
280.0
260.0
240.0
220.0
200.0
180.0

J.

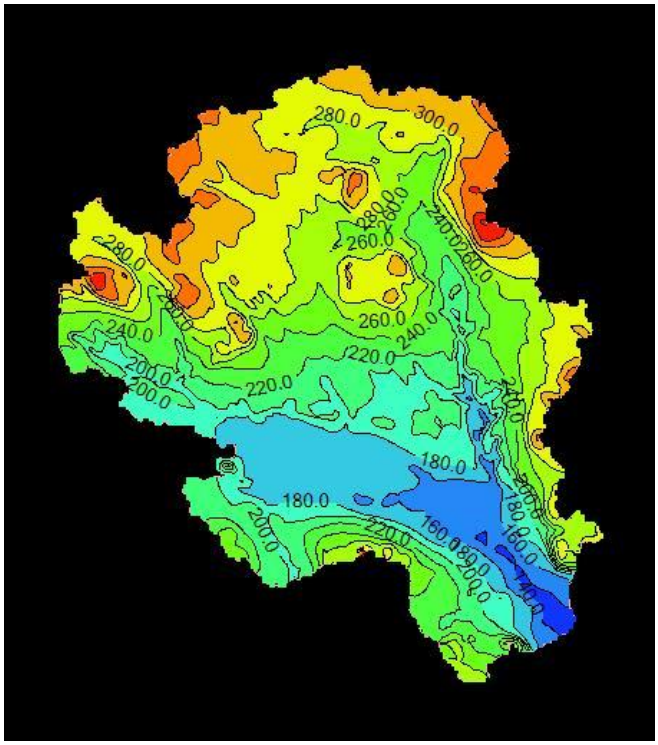
300.0
280.0
260.0
240.0
220.0
200.0
180.0

K.

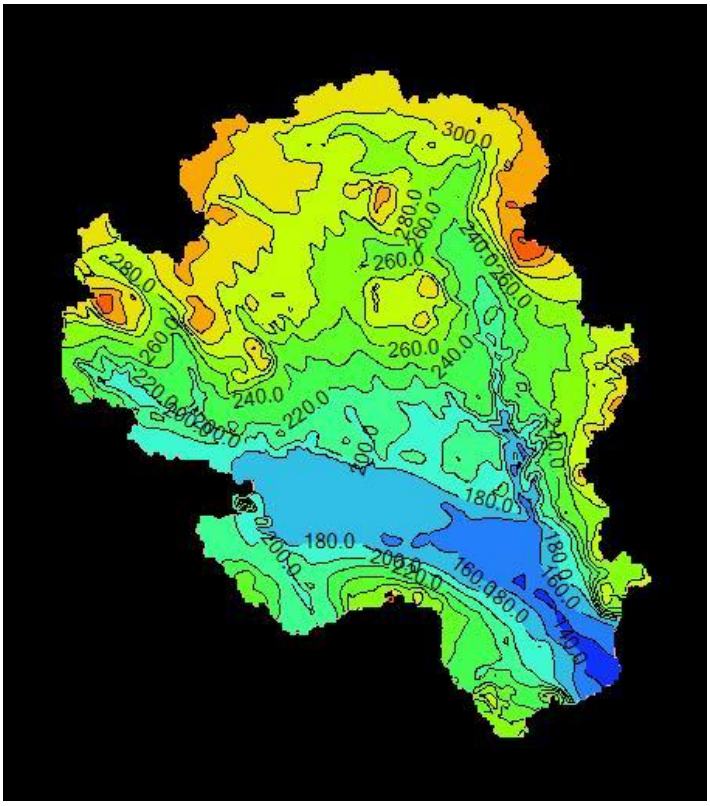

L.

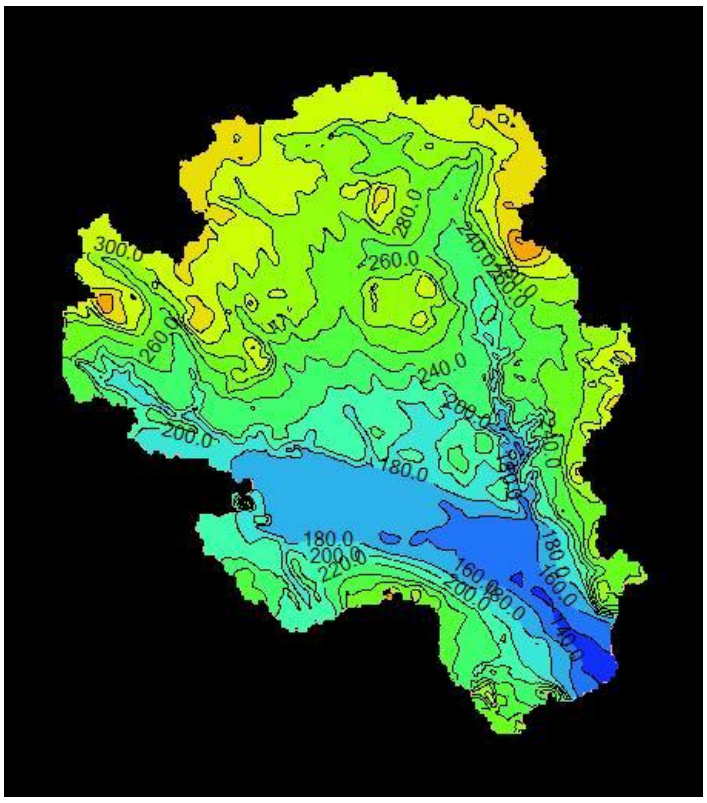

Figure A-2: Water table elevation maps of each month of 2019

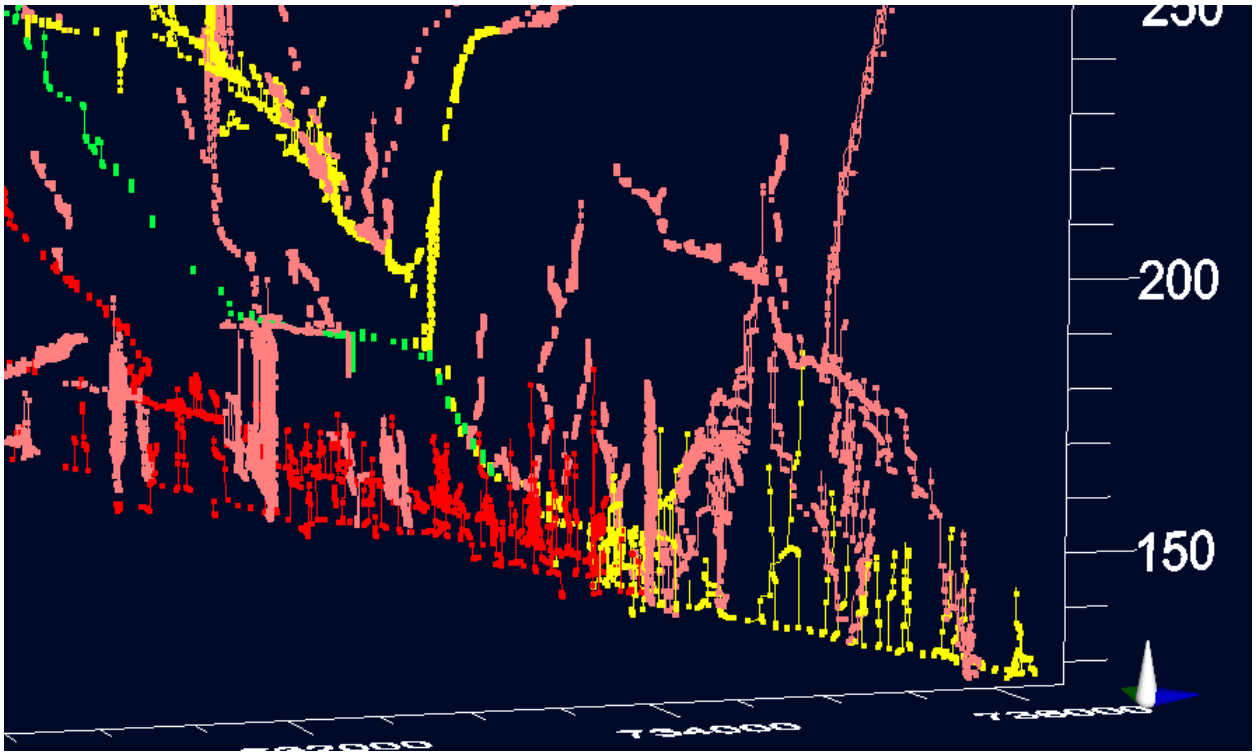

Figure A-3: Pathlines of the river particles (zoomed in)